united nations
educational, scientific
and cultural
organization

international atomic
energy agency

the
abdus salam
international centre for theoretical physics

SMR: 1133/23

WINTER COLLEGE ON
SPECTROSCOPY AND APPLICATIONS

(8 - 26 February 1999)

"A Review of Recent Advances in Semiconductor Laser Based Gas Monitors"

presented by:

Peter WERLE
Fraunhofer Institut für Atmosphärische Umweltforschung
Kreuzeckbahnstr. 19
D-82467 Garmisch-Partenkirchen
Germany

These are preliminary lecture notes, intended only for distribution to participants.

strada costiera, 11 - 34014 trieste italy - tel. +39 40 2240111 fax +39 40 224163 - sci_info@ictp.trieste.it - www.ictp.trieste.it

ELSEVIER

Spectrochimica Acta Part A 54 (1998) 197–236

SPECTROCHIMICA ACTA PART A

Review article

A review of recent advances in semiconductor laser based gas monitors

Peter Werle

Fraunhofer Institut für Atmosphärische Umweltforschung, Kreuzeckbahnstr. 19, D-82467 Garmisch-Partenkirchen, Germany

Received 18 July 1997; received in revised form 21 August 1997; accepted 15 September 1997

Abstract

When first tunable diode lasers were developed in the mid-1960s they found immediate application as much needed tunable sources for high-resolution laser absorption spectroscopy commonly referred to as TDLAS (tunable diode laser absorption spectroscopy). Substantial improvements in sensitivity and detection speed have been achieved since then and an increasing number of laser based gas monitoring applications has been reported. Diode lasers in general continue to find application to research areas requiring very high resolution, accuracy and sensitivity. In this article the main features and applications of tunable diode laser absorption spectroscopy will be reviewed. The main characteristics of the currently available semiconductor diode lasers with respect to spectroscopic applications and sensitive detection techniques will be discussed. The focus will be on high frequency modulation schemes, which have been developed and utilized for a series of gas monitoring applications in the past. Recent approaches in sample modulation enhanced high frequency modulation spectroscopy developed to cope with limitations caused by signal instability will be addressed together with the future perspectives of TDLAS. © 1998 Elsevier Science B.V. All rights reserved.

Keywords: Semiconductor laser based gas monitors; Tunable diode lasers; Laser absorption spectroscopy

1. Introduction

In the past, gases were monitored in manufacturing plants almost entirely for safety and pollution control purposes. As such gas monitoring was seen as an unwelcome but unavoidable cost item. But, over the last few years, the sophistication of these processes has increased, requiring a growing use of gas analysis as a vital control tool for manufacturing processes. Gas analysers have recently been developed which meet the requirements for faster, more specific and precise measurements. The need to meet increasingly stringent environmental and legislative requirements has also led to the development of analyzers to measure concentrations of a variety of gases. Beside the non-dispersive infrared technique (NDIR), correlation spectrometers and dispersive systems for spectral gas analysis, laser based analysis techniques are at the threshold of

1386-1425/98/$19.00 © 1998 Elsevier Science B.V. All rights reserved.
PII S1386-1425(97)00227-8

routine applications in environmental monitoring and industrial process gas analysis. So far the development of this technology has been driven mainly by scientific questions, but increasingly these techniques are applied to a sensitive, selective and fast analysis for industrial and monitoring applications. The current instrumentation for gas analysis is mainly characterized by a variety of different technologies which are applied for different gases: ozone is monitored with UV-photometers, for hydrogen peroxides and formaldehyde a derivatisation technique (chemical technique with fluorometric detection) is applied, SO, measurements are based upon fluorometric techniques and nitrogen oxides (NO,, NO,) are measured by chemiluminescence. This variety makes system integration difficult, requires many different calibration procedures and increases maintenance costs. As the number of substances to be measured increases continuously, multicomponent analyzers allowing the simultaneous measurement of different gases or pollutants, are required because such systems will be more cost effective and flexible than systems based on individual analyzers. For the variety of problems, different measurement techniques can be applied, but especially optical and spectroscopic techniques attain increasing attention for fast and selective on-line measurements. Differential optical absorption spectroscopy (DOAS) is mainly used for integral measurements over long optical paths in the atmosphere. Light detection and ranging (LIDAR) is applied to remote sensing applications. While Fourier transform infrared spectroscopy (FTIR) is ideally suited for multicomponent analysis and for spectral analysis of unknown gases, laser spectroscopy is a method of choice for in-situ trace gas analysis, because of its much higher sensitivity and specifity due to its higher spectral resolution.

When lead-salt tunable diode lasers (TDL) were first introduced in the mid-1960s they found immediate application as much needed tunable sources for high-resolution infrared laser absorption spectroscopy. According to Beer's law the most important application of TDLs to atmospheric measurements has turned out to be their use in conjunction with a long-path cell to provide high sensitivity local measurements. This technique is commonly referred to as TDLAS (tunable diode laser absorption spectroscopy) and forms the main concern of this article. Substantial progress in various techniques and components has been made in the past and an increasing number of applications has been reported. Tunable lasers in general continue to find applications in research areas requiring very high resolution, specificity, accuracy and sensitivity. In this review article the main features and applications of TDLAS will be summarized. After a brief discussion of the main characteristics of the currently available semiconductor diode lasers with respect to spectroscopic applications, sensitive detection schemes in TDLAS will be discussed. The focus will be on high frequency modulation schemes which have been developed and utilized for a series of applications during the last few years. Finally, recent approaches to cope with stability problems and the future perspectives of TDLAS will be addressed.

2. TDLAS

TDLAS usually scans over an isolated absorption line of the species under investigation using a single narrow laser line. To achieve the highest selectivity, analysis is made at low pressure, where the absorption lines are not substantially broadened by pressure. This type of measurement was pioneered by Hinkley [1] and Reid et al. [2], and has developed into a very sensitive and general technique for monitoring most atmospheric trace species [3 - 16]. The main requirement is that the molecule should have an infrared line-spectrum which is resolvable at the Doppler limit, which in practice includes most molecules with up to five atoms together with some larger molecules. The intensity of monochromatic laser radiation of frequency ω transmitted through a sample cell containing an absorbing species is given by Beer's law

$$I(\omega) = I_0(\omega)\, e^{-\sigma(\omega)LN} \quad (1)$$

where I_0 is transmitted intensity in the absence of an absorbing species, L is the optical path length

within the cell, a(w) is the absorption coefficient and N is the concentration of the absorbing species in molecules per unit volume. The cell absorbance is defined by $a = \sigma(\omega)LN$. A given molecular absorption line is characterized by its integrated line strength S, which is independent of pressure, while the lineshape depends on sample pressure. At atmospheric pressure, in the mid infrared collision broadening dominates giving a Lorentzian lineshape. As the sample pressure is reduced, the pressure broadened linewidth decreases until, at pressures below a few millibars, Doppler broadening dominates and the lineshape becomes Gaussian. The optimum sampling pressure for TDLAS is a compromise between sensitivity and selectivity. As the sampling pressure is reduced sensitivity does not fall significantly below the atmospheric pressure value until the point at which Lorentzian and Doppler linewidths are equal at typical pressures of 10-50 mbar. This is the pressure at which a TDLAS system is normally operated. In this pressure range the lineshape can be described as a convolution of Lorentzian and Doppler line shapes known as the Voigt profile. The Voigt profile tends to the Lorentzian profile at high pressure and to the Doppler at low pressure and is thus the general form of the line shape. Because TDLAS operates at reduced pressure it is not restricted in wavelength to the so called atmospheric windows such as 3.4-5 μm and 8 - 13 μm. However operation outside these windows is not always possible due to the absorption in the tailing of strong H_2O or CO, lines. This is not normally a problem because the sharp target gas absorption line is easily distinguished from a broad tailing of strong interfering lines. When operating in the non-window regions one has also to consider broad absorptions, due mainly to water vapour, which can occur in the optical path at ambient pressure outside of the multipass cell. These can attenuate the laser power incident on the detector and cause a drifting background spectrum.

Conventional direct absorption measurements have to resolve small changes in a large signal. In comparison with direct spectroscopy, the benefits of modulation spectroscopy in TDLAS are 2-fold. Firstly, it produces a difference signal which is directly proportional to the species concentration (zero baseline technique) and, secondly, it allows the signal to be detected at a frequency at which the laser noise is significantly reduced. Wavelength modulation spectroscopy (WMS) has been used with tunable diode laser sources since the early 1970s. The earliest TDL systems used a modulation frequency in the lower kHz range and second harmonic detection. Today 50 kHz modulation with 100 kHz detection is quite usual and, consequently, it is convenient to regard 100 kHz as the limit of conventional wavelength modulated TDLAS. Modulation spectroscopy is based on the ease with which diode lasers can be modulated. In WMS with diode lasers, the injection current is sinusoidally modulated as the laser wavelength is tuned through an absorption line. When the laser is modulated around its center frequency ω_L at a frequency ω_m, the instantaneous frequency is $\omega = \omega_L + \delta\omega \cos(\omega_m t)$, where $\delta\omega$ is the modulation amplitude, typically of the order of the absorption linewidth. The modulation frequency ω_m is typically below 50 kHz. The intensity $I(\omega_L)$ of the radiation transmitted through the absorption cell can then be expressed as a cosine Fourier series:

$$I(\omega_L, t) = \sum_{n=0}^{\infty} A_n(\omega_L) \cos(n\omega_m t) \tag{2}$$

The individual harmonic components A_n (for $n > 0$) can be measured with a lock-in amplifier and are given by:

$$A_n(\omega_L) = \frac{2}{\pi} \int_0^{\pi} I_0(\omega_L + \delta\omega \cos 0) \exp[-\sigma(\omega_L + \delta\omega \cos\theta) LN] \cos n\theta \, d\theta \tag{3}$$

where θ has been substituted by $\omega_m t$. Eq. (3) can be evaluated provided $I_0(\omega)$ and $\sigma(\omega)$ are known. In the ideal case the absorption line can be scanned without any change in I_0 and Eq. (3) becomes:

$$= \frac{2I_0}{\pi} \int_0^{\pi} \exp[-\sigma(\omega_L + \delta\omega \cos\theta)\, LN] \cos n\theta \, d\theta \quad (4)$$

In the limit of low absorbance, $\sigma LN \ll 1$, which is true for trace gas detection at the part-per-billion level, this becomes

$$A_n(\omega_L) = \frac{2I_0 NL}{\pi} \int_0^{\pi} -\sigma(\omega_L + \delta\omega \cos\theta) \cos n\theta \, d\theta \quad (5)$$

Thus each harmonic component is directly proportional to the species concentration N. A special case occurs when the modulation amplitude $\delta\omega$ is much smaller than the absorption linewidth. In this case, a Taylor series expansion of $\sigma(\omega)$ gives:

$$A_n(\omega_L) = \frac{I_0 2^{1-n} NL}{n!} \delta\omega^n \left.\frac{d^n\sigma}{d\omega^n}\right|_{\omega=\omega_L} \quad (6)$$

Here the nth harmonic component is proportional to the nth derivative of a(w) and the technique is known as 'derivative' or wavelength modulation spectroscopy [4,5]. This small modulation regime is never used in practice because of its low sensitivity. In practical applications $\delta\omega$ is made close to the linewidth in order to maximize the signal amplitude. It turns out that even in this case the signal is qualitatively similar to the nth derivative of the absorption lineshape [17]. In general, one can monitor signals at all harmonics of the modulation frequency, although usually only the first and the second-harmonic signals are used. These signals are roughly proportional to the first and second derivatives of the absorption line shape. The normal mode of operating a TDLAS system is to scan the laser center frequency ω_L through the absorption line repeatedly at about 100 Hz and use a computer-controlled signal averager to accumulate the signal from the lock-in amplifier which is measuring $A_n(\omega_L)$. This produces a harmonic spectrum of the line, the amplitude of which is proportional to the species concentration. Scanning over the line gives increased confidence in the measurement because the characteristic feature of the measured species is clearly seen and unwanted spectral features due to interfering species or etalon fringes can easily be identified. Advances in data-processing technology have allowed increasingly faster data acquisition rates to be used. The use of higher averaging rates allows considerable improvement in the ultimate signal-to-noise ratio. This technique provides the advantage of the unambiguous detection of the target gas by comparison of the measurement with the calibration structure. Since the amplitudes of all harmonics are proportional to species concentration, each of them can be used for monitoring. In practical TDLAS systems, where a sample cell operating at reduced pressure is used, the second harmonic is efficient to eliminate linear slopes of the spectra and is the most favourite one.

A typical mid-infrared TDLAS system for the spectroscopic detection of an individual atmospheric species in the ppbv range is shown in Fig. 1a. The whole optical setup is mounted on a 1 x 0.6 m optical breadboard and should be enclosed in a box to improve the thermal stability. A lead-salt diode laser is housed in a liquid-nitrogen (LN,) cooled dewar. To accommodate a possible deviation angle between the cone of laser emission and the laser mount axis, the LN_2-dewar is mounted on a xyz-stage alignable within + 30°. The beam from the TDL is first collimated by an off-axis paraboloid (OAP) and then directed by a sequence of mirrors through the sample cell and onto a LN_2-cooled HgCdTe (MCT) photovoltaic detector. A visible 670 nm laser beam is combined via a pellicle beam splitter with the invisible infrared beam to assist in alignment. Because of low transmission in the infrared, the pellicle beam splitter is kinematically mounted and can be removed during the trace gas measurements. Typical line-strengths are such that an atmospheric concentration of 1 ppbv produces an absorption of only 1 part in 10^7 over a 10 cm path length. Conventional absorption spectroscopy techniques will clearly not be able to measure such small absorptions. TDLAS overcomes this problem by using a multi-pass cell with path lengths of 100 m or more. Such cells achieve the long path by using mirrors to fold the optical path, giving typically 100 passes of a 1 m base-length cell. The design requirements for the multipass cell are long total

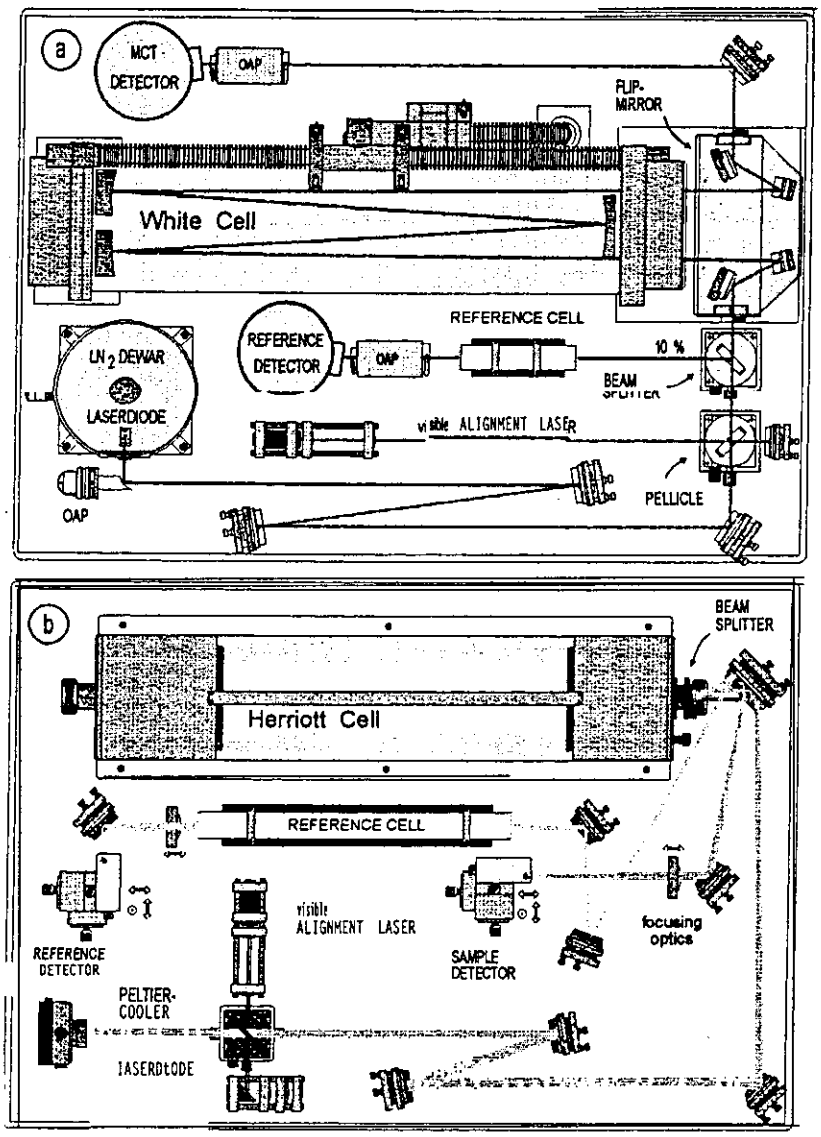

Fig. 1. Opto-mechanical layout for a typical (a) mid infrared tunable diode laser absorption spectrometer operating at cryogenic temperatures of the laser and detectors and (b) a near infrared system based on Peltier cooled devices.

pathlength to give high sensitivity, low volume to give a fast response time and to allow rapid alternation between sample and background spectra. Two basic designs of cells are most commonly used in TDLAS instruments: White [18] and Herriott cells [19]. A commercial White cell module (Miitek MDS 1600) developed at the Fraunhofer Institute for Physical Measurement Techniques (Freiburg, Germany) with base length 62.5 cm and focusing optics is shown in Fig. la. It has a volume of 61 and a usable pathlength of 100 m. Zero astigmatism can be achieved by appropriate choice of the vertical separation of the tow rows of spots on the field mirror. A second system using a Herriott cell and designed for near-infrared spectroscopy is displayed in Fig. lb. The

principal setup is the same as for the mid-infrared system. As no cryogenic cooling is required the thermoelectric cooled laser mounts and detectors are significantly smaller. In this system design a commercial Herriott type multipass absorption cell (New Focus 5612) developed by Aerodyne Research (Billerica, MA) has been integrated. This Herriott cell consists of two spherical mirrors separated by approximately their radius of curvature [20]. The optical beam is injected through a hole in one mirror and is reflected back and forth a number of times before exiting from the same hole. The images normally occur in the middle region of the cell, so the beam size at either mirror is smaller than in the White type cell of the same base length. In the original design the beam traces out elliptical paths on the two mirrors, however this does not properly use the mirror area and thus a modified arrangement using slightly astigmatic mirrors has been used recently [21]. In this case the beam traces out a Lissajous figure. An advantage of the Herriott cell over the White cell is that it is easy to align, since the output beam direction is insensitive to 'changes in the mirror alignment. A significant disadvantage is that the number of passes is determined by the mirror separation and it is difficult to make this adjustable in any given cell design.

Most TDLAS systems are limited in sensitivity by optical fringes superimposed on the measured spectrum. These result from unwanted etalons formed by reflections and scattering in the optical system. The fringes take the form of an approximately sinusoidal variation of the background signal with a period equal to the free spectral range of the etalon. These fringes can be reduced by careful optical design and adjustment, but it is usually difficult to reduce the fringe amplitude to a level much below that equivalent to an absorbance of 10^{-4}. In order to achieve sensitivities in the 10^{-5}–10^{-6} range further methods of reducing the effect of the fringes have to be found. Precautions to reduce the etalon formation include the use of reflective optics where possible, wedging and angling of all windows and antireflection coating of window and lens surfaces. Accurate alignment of the TDLAS optical system is important in avoiding optical fringing and is difficult to achieve due to the invisibility of the beam in infrared systems. As the most critical element with respect to etalon formation, the laser collimating lens has a difficult task since it must cope with the divergent beam from the laser. An $f/1$ off-axis paraboloid mirror is commonly used for this.

An important function of the laser control system is to lock the laser frequency to the absorption linecenter. This is usually achieved by splitting off part of the beam by a BaF, window and directing it through a line-locking cell onto a reference detector. The reference cell is filled with the target gas at a pressure of typically a few millibars in order to give a strong signal at high signal-to-noise ratio. The first harmonic signal from this cell is usually detected with a phase sensitive lock-in-amplifier. This signal has a zero crossing at line center and can thus be fed back to the laser current/temperature controller to lock the laser to the line. This gives short term stabilization of the laser wavelength but can be subject to diurnal drifts of the control electronics. The position of the reference signal is therefore continuously monitored by the computer and any shift is corrected by a control signal to the laser current controller. The technique just described uses feedback control of the laser current. However in most cases it is drift of the laser temperature which is the main cause of wavelength drift. The disadvantage of using current control to compensate for temperature drift is that although the wavelength is controlled, the laser intensity may vary. It is therefore better to use feedback control of the laser temperature if the design of the temperature controller allows this.

TDLAS systems are usually calibrated by target gas mixtures of known concentration and, therefore, it is often not necessary to know exactly which absorption line is being monitored. When using a laser which is specified to operate in the selected wavelength range the normal procedure is to vary the laser temperature and drive current until a strong signal is seen with a reference cell inserted in the beam. The best and most direct calibration method is to sequentially attach calibrant and zero air sources to the instrument inlet. This method has the advantage of calibrating the

entire signal processing chain. In general, oven-stabilized permeation sources are preferred although dilution of standard gas mixtures can be used. Ideally zero air should be obtained by scrubbing from the ambient air only the species being monitored. In this way the background spectrum will contain any interferences from other atmospheric species, and these will then be subtracted from the sample spectrum. Zero air should contain levels of the monitored species well below the required detection limit since all measurements will be relative to this zero air level. Because of the linearity of the TDLAS technique at low optical densities usually a single point calibration is sufficient. Even when measuring very high concentrations linear response can always be achieved by either using a shorter path-length or a weaker absorption line. In principle TDLAS measurements can be calibrated absolutely using the known absorption line strength and line profile at a given pressure for systems using sweep integration. Modulation techniques complicate the use of calculated absorptions and, consequently, the absolute optical calibration is rarely used. However, it is used to check for optimum operation of the instrument.

The factors involved in choosing the absorption line suitable for trace gas monitoring are: a strong line is needed to achieve high sensitivity. Because the tuning range of a diode laser is not always continuous the strongest absorption line might not be accessible. Even where a diode is specified to be initially capable of operating at a particular wavelength its characteristics can easily change over time. Therefore, it is important to choose a wavelength with several strong lines within the tuning range of the laser so that there is a high probability that at least one strong line will always be accessible. The line should, if possible, be isolated from other lines of the same species, but this is not an absolute requirement and can prove difficult to be achieved for larger molecules. The line should be isolated from interfering lines due to either other trace species or the more abundant atmospheric constituents such as H_2O. The latter causes most of the problems because it absorbs over a large part of the infrared region. Water vapor content in the atmosphere has a relatively high and variable concentration, which results in even weak lines producing significant absorption. The task of choosing the operating wavelength is made easier by the existence of spectral-lines databases of which the most popular is the HITRAN compilation. This currently covers more than one million transitions and includes for example data on CO, CO_2, N_2O, CH_4, O_2, SO_2, H_2O, NO, NO_2, NH_3, HNO_3, H_2O_2, HCHO, HF and HCl. Wavenumber, line strength and Lorentzian halfwidth are available for each line. The database is available on CD-ROM together with a database software to plot synthetic spectra for user specified gas mixtures at any temperature and pressure.

In multicomponent applications a separate laser is usually required for each species because of the limited tuning range of individual lasers. In the most common approach the collimated beams from these lasers are sequentially directed along the optical path through the instrument by either a rotating selecting mirror on a galvanometer drive or by individual 'pop-up' mirrors for each laser. While this time multiplexing method does not provide true simultaneous measurement, it is possible to cycle through four species within less than a minute, which is almost simultaneous. Within the data-processing system the spectra of the individual species are accumulated separately over the required averaging period. However, because the duty cycle of each laser is reduced by multiplexing, a longer total period is needed to achieve a given sensitivity compared to the equivalent single-species measurement. A further potential disadvantage is that line-locking is not continuously maintained for each laser so loss of lock could occur for slow cycle times or with poor temperature stabilisation of the lasers. When using modulation spectroscopy a possible alternative technique is to permanently combine the laser beams and use different modulation frequencies and lock-in amplifiers for each laser. Although this appears attractive at first sight, the main disadvantage is that the single detector sees the noise of all the lasers, so the SNR is degraded. This is particularly unfavourable, when the lasers have widely different powers, as frequently happens. The signal from the lowest power laser is

then likely to be overwhelmed by the noise from the other lasers. Fried et al. have shown that where two species have suitable lines within the current tuning range of a single laser both can be measured simultaneously using a technique known as jump scanning [22]. The normal low frequency ramp through the line is replaced by a ramp which first sweeps through the line of one species and then jumps discontinuously by adding a dc current offset before sweeping through the line of the second species. The spectra of the two species are thus acquired quasi-simultaneously and appear as adjacent lines on the spectrum. These can be then analysed separately. The number of pairs of species which have suitable close and strong line is quite limited; examples are nitrogen dioxide and ammonia at 1625 cm^{-1} and nitric acid and formaldehyde at 1720 cm^{-1}. For this special application the laser must access both lines within the same current scan and deliver strong, noise-free and single-mode output at both.

Many applications of TDLAS have been presented in the literature. Most applications have been reported in the field of atmospheric research [23-36], where still better and faster instrumentation is required. Examples are the investigation of the temporal development of spatially distributed polluted air masses from airborne platforms such as balloons or aircraft and the determination of trace gas fluxes (deposition and emission) in terrestrial ecosystems by means of the eddy correlation method [37-41]. Many of these applications require instruments with higher temporal resolution and better sensitivities. While some years ago the use of tunable diode laser absorption spectroscopy for atmospheric measurements dominated the application this has changed in recent years. With the increasing complexity of chemical processes, online gas analysis is becoming a key issue in automated control of various industrial applications and the application of tunable diode lasers in industrial monitoring is becoming more and more important. Besides important scientific applications in molecular spectroscopy [42-45], low temperature studies [46-48] and plasma analysis [49-51], diode lasers gain increasing interest in combustion diagnostics [52-56], investigations of aero engines and automobile exhaust measurements [57-61]. In the pharmaceutical industry, accurate control of oxygen or carbon dioxide levels is often crucial to the efficiency, or even the viability of processes [62-65]. There are many interesting medical applications [66-72] as for example time resolved gas analysis or isotopic ratio measurements in human expiration breath. Other challenges are the online analysis of high purity gases [73-75], detection of explosives [76-78] or pollutant monitoring applications in the aluminium industry [79,80].

The major features of TDLAS rendering it such a valuable technique for gas analysis are: (a) it is specific and as a high resolution spectroscopic technique it is virtually immune to interferences by other species-a problem that plagues most competing methods. This ability to provide unambiguous measurements leads to the use of TDLAS as a reference technique against which other methods are often compared. (b) It is a technique universally applicable to all smaller infrared active molecules and the same instrument can easily be converted from one species to another bychanging the laser and calibration gases. Because of this feature it is easy to construct an instrument which will measure several species simultaneously by multiplexing the outputs of several lasers through the multi-pass cell. (c) It is fast and sensitive. The time-resolution of TDLAS measurements can be traded off against sensitivity and this allows very fast measurements with millisecond time resolution. The main disadvantages are the complexity and the cost of TDLAS instruments as well as the need for expert operators. Despite the success of TDLAS in many applications there are still problems to solve. Most of them are connected with the properties of the diode laser, which are thus the most critical component of the TDLAS systems. The properties of these devices are considered in the next section.

3. Semiconductor lasers for spectroscopic applications

Despite the many advantages of diode laser absorption spectroscopy, the technique has not yet found widespread application in industrial

process control. The reasons for this are found in the relative complexity of current instrumentation and the lack of high quality, high power diode lasers for the spectral regions of interest. A main drawback for industrial applications of laboratory prototype spectrometers is the limited suitability of the currently available lasers for continuous operation in an industrial environment. Operational cost is frequently too high, lifetime too short and the system might be too vibration sensitive. In analogy to the historical development of commercial radio systems from valve-sets to semiconductor technology we observe a similar process in laser technology, and near infrared semiconductor lasers are a typical example. They are widely used in communication and consumer electronics, which has led to a highly sophisticated level of manufacturing technology, and availability in high quantities at low costs meets the requirements of industrial applications. However, because of the small number of application, middle IR diode lasers are still produced in small batches and on a much lower level of manufacturing sophistication.

Common commercial diode lasers, made from the III-V group of semiconductor materials, emit at red and near infrared wavelengths from about 0.63-1.55 μm. This includes the InGaAsP/InP 1.3- 1.55 μm optical communication lasers, as well as the GaAs/AlGaAs 0.78 and 0.83 μm lasers found for example in compact disk players. The technology of near-IR 1.3 - 1.55 μm InGaAsP/InP diode lasers developed for fiberoptic communication can be extended to fabricate lasers that emit anywhere in the wavelength interval of about 1.2- 1.8 μm. The device structures are multiple-quantum-well distributed-feedback (DFB) lasers. Lasers operating in this spectral region are fabricated at the David Sarnoff research Center (Princeton, NJ) and have been used at SRI (Menlo Park, CA) to detect, e.g. CO, and CO at 1.6 μm and CH, at 1.65 μm [81,82]. Near-IR diode lasers have the advantages of single-mode outputs at milliwatt power and near-room-temperature operation in addition to the availability of fiberoptic technology and inexpensive auxiliary equipment such as thermoelectric coolers, collimating lenses, optical isolators, low noise current drivers and detectors. Near-IR lasers are compact and show long lifetimes and a high electro-optical conversion efficiency. Of special interest for spectroscopic applications is the fast tunability of the laser emission wavelength and the high spectral resolution. Together with sophisticated noise suppression schemes they allow highly sensitive spectroscopic gas analysis. The availability of single-mode diode lasers will lead to many applications based on molecular spectroscopy. One significant drawback of these devices is that they are available only in very narrow spectral regions and most vendors are either unable or unwilling to provide wavelength-selected diode lasers for spectroscopic applications. This situation, however, is changing. Another drawback of near-IR diodes is that only a limited number of molecular species have absorption features in the spectral region covered by these lasers. Furthermore, the near-IR absorptions are overtone or combination bands that are typically one to several orders of magnitude weaker than the IR-fundamental band. Nevertheless, many molecules of interest have near-IR absorption bands that are strong enough for detection at parts-per-million (ppm) and, in some cases, even parts-per-billion (ppb) levels.

For wavelengths longer than 1.8 μm, III-V diode lasers can be made from antimonide containing compounds such as AlGaAsSb, InGaAsSb, and InAsSbP. Room temperature lasing from 2-2.4 μm has been reported from simple double heterostructure antimonide diode lasers. As wavelength increases up to 3.7 μm, the maximum operating temperature decreases as a result of increasing optical and electrical losses. Meanwhile the first devices around 2 μm are commercially available from Sensors Unlimited (Princeton, NJ). Recently III-V devices based on InAsSb/InAsSbP manufactured at the Ioffe Physic0 Technical Institute (St. Petersburg, Russia) have been investigated with respect to spectroscopic applications [83]. These double heterostructure devices were grown by liquid phase epitaxy on InAs substrate and cover the spectral range from 2.7-3.7 μm at LN, temperatures. A detailed characterization and measurements at the Fraunhofer Institute IFU (Garmisch-Partenkirchen, Germany) have shown

that these devices are well suited for the detection of HCHO at 3.4/3.6 μm and CH, at 3.26 μm [84,85]. Especially the single mode power of more than 1 mW is very attractive for spectroscopic trace gas monitoring. Nevertheless careful selection of laser devices is necessary and, therefore, future work has to be done to improve the manufacturing process and the quality of this novel devices, which look very promising for sensitive gas analysis.

Diode lasers, made from IV-VI (lead-salt) semiconductor materials, operate in the 3-30 μm spectral region and, therefore, they cover the IR fundamental band with strong absorptions for the most atmospheric trace gases. They are used almost exclusively for spectroscopic applications. Because IV-VI lasers and their associated detectors operate at cryogenic temperatures, they are more expensive and more cumbersome to use than III-V devices. Lead-salt diode lasers have been used to determine molecular parameters for IR absorption spectra and for high-sensitivity trace gas detection using molecular fundamental band absorptions. In the trace gas monitoring applications, lead-salt laser instruments have routinely achieved ppb detection levels of a number of important molecular species. Such instruments have been used for atmospheric research and for combustion diagnostics. For many industrial application, however, the use of lead-salt diode lasers is limited by the need of cryogenic cooling, frequent multimode emission and power levels which are typically only several hundred microwatts. At present lead-salt diodes suitable for cw operation in the mid-infrared are manufactured by Laser Analytics (Andover, MA) and by Laser Components (Olching, Germany). Both manufacturers are actively developing new types of diodes that will very welcome in the TDLAS community. Unfortunately, the high quality lead-salt laser diodes from Fujitsu in Japan are no longer available.

Lead-salt tunable diode lasers are similar in principle to the more familiar GaAs semiconductor lasers. The simplest form consists of a crystal of a lead-salt semiconductor such as $Pb_{1-x}Sn_xSe$ on which a p-n junction is formed by diffusion of a salt of different stoichiometry into the top surface. The crystal is cleaved to a chip about 300 μm long with front and rear faces about 100 μm square. These front and rear facets form the laser cavity and do not need any reflective coating as the Fresnel reflection is sufficiently strong. If electrodes are deposited on the top and bottom surfaces and a current of a few hundred mA passed through the junction, lasing action takes place at a wavelength determined by the semiconductor energy gap. This energy gap is temperature dependent and typical lasers can be temperature tuned over about 100 cm^{-1}. The energy gap is also dependent on alloy composition so that lasers of different wavelength can be obtained either by varying the stoichiometry of the salt or, for wider tuning, by using different constituents, e.g. PbSnTe or PbSSe. The simple laser just described is known as a diffused homojunction laser and has many disadvantages such as poor mode structure, low power, and the need to operate below liquid nitrogen temperatures. Now that lasers operating above 77 K are available at most wavelengths, temperature-controlled liquid-nitrogen dewars are the cooling method of choice. However where long term unattended operation is needed, or where LN_2 supplies are not available, miniature Stirling cycle coolers, developed for space applications and capable of cooling to LN_2 temperatures, can be attractive. The ultimate goal in increasing laser operating temperatures is to allow the use of thermoelectric coolers. Lasers in current production have more sophisticated structure and those intended for operation above 77 K are the first choice for any new TDLAS system because of their simpler cooling needs. They are of double heterostructure (DH) or buried heterostructure (BH) construction and are formed by molecular beam epitaxy (MBE) with PbEuSeTe or PbSnTe active layers. The lasers are normally specified for operation up to about 120 K. Lasers of this type are typically available between 3050 and 900 cm^{-1} with single-mode operation available over much of this range. Powers are typically 200 μW but single-mode lasers with powers of 1 mW can be produced at most wavelengths. For reviews of lead-salt TDLs see Eng et al. [86], Preier et al. [87], Wall [88], Tacke [89,90], Feit et al. [91,92] and Shotov et al. [93].

Compared to GaAs lasers, lead-salt semiconductor lasers are at a relatively early stage in their development due to the much smaller market. Current development is aimed at better mode quality, higher power and higher temperature operation. Various routes are being explored including buried quantum well (BQW) structures, and laser cavities employing distributed feedback (DFB) and distributed Bragg reflectors (DBR). In the quantum well design the thickness of the active layer is reduced to 100 nm resulting in quantization of the valence and conduction band energy levels. The lasers have predominantly single-mode characteristics and higher efficiency as a result of the quantum effects, and can have higher power and higher operating temperature than conventional structures. The DFB and DBR cavity designs use corrugated structures, either distributed along the entire cavity (DFB) or at each end (DBR). Due to the Bragg condition these structures act as distributed or discrete reflectors but only at specific wavelengths. They thus give additional control over the laser modes and can give predominantly single-mode operation.

TDLS are tuned by varying the temperature of the active region. This can be done either by varying the temperature of the cold stage on which the diode is mounted or by varying the laser drive current, which varies the Ohmic heating of the active region. Varying the base temperature will tune the laser over its entire range but is slow. Varying the drive current gives a more restricted tuning range, of maybe 20 cm^{-1}, but allows faster modulation of the laser frequency. In practice the two methods are used in combination. Fig. 2a and b show a typical mode map of a lead-salt diode laser at fixed base temperature of 95 K and increasing drive current from 1 00– 350 mA. At a particular drive current the output consists of a series of longitudinal modes separated in wavenumber by $1/2nL$ where n is the refractive index of the active layer (5-6) and L is the cavity length (typically 0.03 cm). Thus the mode separation is about 3 cm^{-1}. It can be seen that the modes are approximately contained within an envelope; the maximum of which tunes with the temperature dependent energy gap of the semiconductor material. The modes themselves tune at a different, slower, rate through the temperature dependence of the refractive index, n, and also through the dependence of n on carrier-density, which varies with the laser drive current. At low modulation frequencies, the temperature variation of n dominates, but at high frequencies ($>$ 1 MHz) thermal inertia reduces the amplitude of the temperature-modulation and carrier-density modulation takes over. A number of important points, common to most lasers, are illustrated by Fig. 2a and b. Laser output is single-mode at low drive current and then becomes increasingly multi-mode at higher currents. An individual mode tunes over about 2 cm^{-1} with power increasing with drive current. There are some wavelengths which are not accessible at all. This can sometimes be remedied by choosing a different combination of base temperature and drive current but frequently the only solution is to use a different laser. Laser mode quality has an important influence on the performance of TDLAS instruments. When starting to use a new laser, the first task is to find a combination of base temperature and drive current at which the laser produces a strong, preferably single mode emission, tuned to the absorption line being monitored. It may be found that the laser characteristics will change with time due to thermal cycling and then the process must be repeated. This problem of the change of the mode structure with age has been a major obstacle for the widespread use of TDLAS, and the properties of the lead-salt lasers presently available have to be substantially improved. One of the aims of current laser development is to achieve simpler more reproducible mode behaviour. A single mode operation is required to minimize mode partition noise and to prevent absorption signals from other modes interfering with the desired signal from the spectral feature of interest. Semiconductor diode lasers oscillate essentially in several longitudinal modes because the linewidth of the gain spectrum is much broader than the separation between adjacent longitudinal modes. In conventional Fabry-Perot type cavities fabricated by cleaving or chemical etching of the crystal facets, power switching between the longitudinal modes (mode hopping) occurs. Even if the power of a specific longitudinal mode dominates,

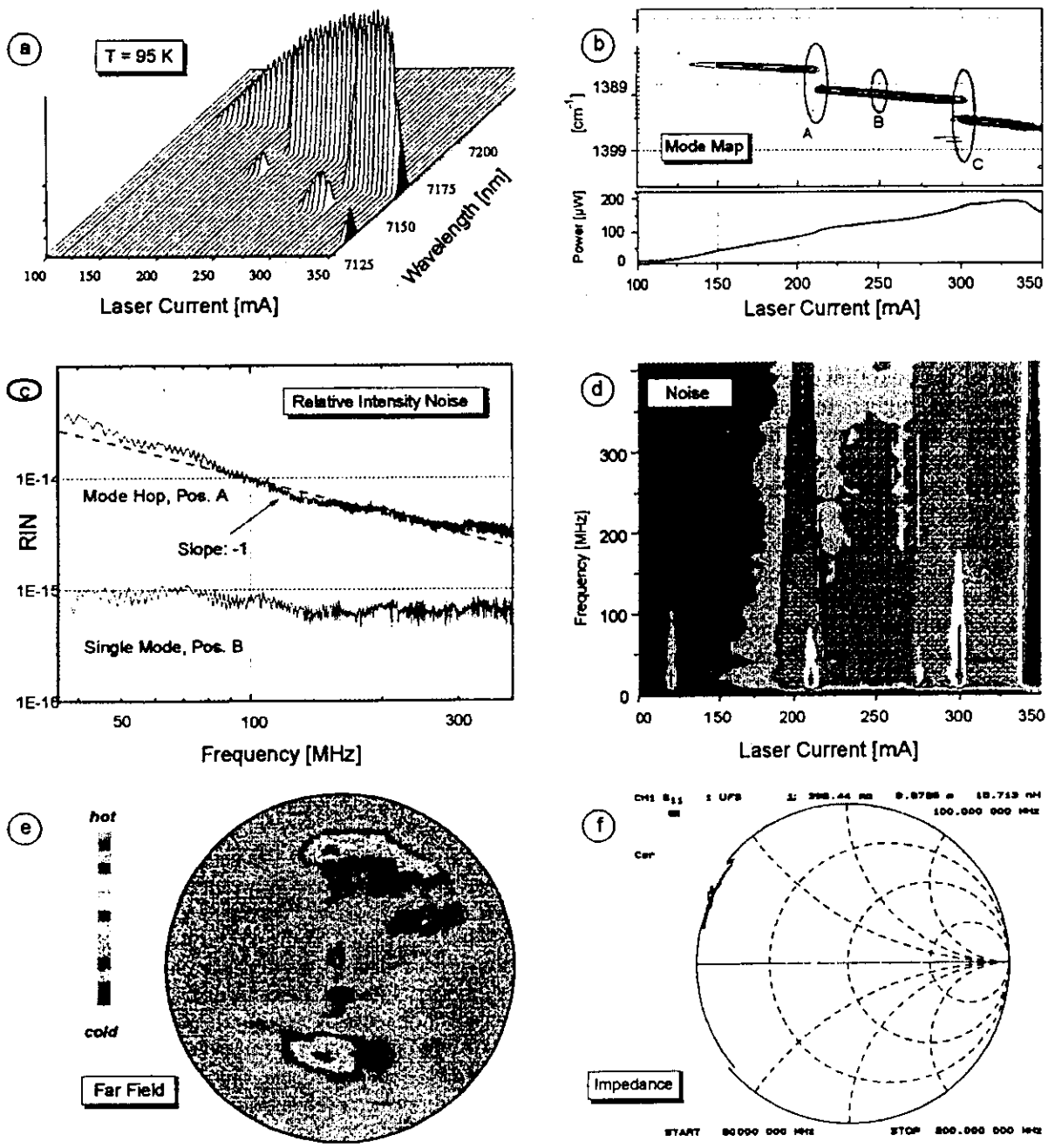

Fig. 2. Summary of typical characteristics of lead-salt diode-lasers: (a) mode map for a fixed temperature fo 95 K (b) tuning characteristics and laser power, (c) relative intensity noise for mode hop position (A) and single mode operation (B), (d) same as (c) but for all currents, (e) laser far field and (f) laser impedance (Smith-chart).

as in the case of a nearly single-longitudinal-mode oscillation, transient decrease of power of the main mode occurs together with an increase in power of the other submodes (mode partition noise).

For sensitive spectroscopic applications the knowledge of the characteristics of laser noise is essential to achieve the optimum system performance. First measurements with lead-salt diode lasers by Eng et al. [94] showed no noise decrease towards higher frequencies due to a limited measurement range. Measurements of wideband noise characteristics of a lead-salt diode laser by Werle et al. in 1989 [95] showed significant $1/f$-type noise contributions up to more than 100 MHz. It was concluded that the application of modulation frequencies beyond that value should lead to a noise reduction of about two orders of magnitude compared to conventional WMS techniques. Many measurements during the past years with different lasers in our laboratory have confirmed these results. In 1991 Fischer and Tacke investigated high frequency intensity noise spectra of mid-infrared lasers with different lateral structures [96,97]. They also found a noise reduction for FM spectrometers at higher modulation frequencies. Such high frequency noise contributions can be attributed, at least in part, to optical feedback effects into the laser [98]. A detailed analysis of noise measurements with single mode lasers, in the vicinity of mode hops and for laser multimode operation showed that the previously stated increase in the noise level at certain operating points can be attributed to mode hopping and mode competition [99]. Fig. 2c shows measurements of the relative intensity noise (RIN) at laser currents corresponding to the mode hop position (A) and the single mode position (B) in Fig. 2b. The complete noise characteristics related to plot 2b is displayed in Fig. 2d. A similar behaviour has been observed with most other lasers and $1/f$-type noise as it can be seen in RIN measurements (Fig. 2c, d) has been attributed to the presence of spurious side modes or even multimode operation. Consequently, higher modulation frequencies are necessary to achieve near shot noise limited performance of a spectrometer with commercial lead-salt diode lasers presently available. Therefore, the use of distributed feedback or distributed Bragg reflector structures seems to be going in a promising direction. It should be mentioned at this point that during recent years specially designed external cavity lasers attained increasing attention due to their broad tuning range [100–105].

A convenient way to describe the sensitivity at a given signal level is the signal-to-noise ratio (SNR). If the noise, and not drift effects in the detection system, is the limiting factor for ultimate sensitivity, the detection limit of a spectrometer can be derived from the signal-to-noise ratio:

$$\mathrm{SNR} = \sqrt{\frac{\langle i_s^2 \rangle}{\langle i_{\mathrm{TN}}^2 \rangle + \langle i_{\mathrm{SN}}^2 \rangle + \langle i_{1/f}^2 \rangle}} \xrightarrow{q.l.} \sqrt{P_{\mathrm{D}}} \propto \sqrt{N_{\mathrm{Ph}}} \tag{7}$$

where P_{D} is the laser power impinging upon the detector and N_{Ph} is the corresponding number of photons. In modulation spectroscopy the *signal* is directly proportional to the laser power incident on the detector, in the mode being absorbed. The three main noise currents to be considered are the thermal noise (TN) of the detector-preamplifier combination, the quantum (shot) noise (SN) and a $1/f$-type laser excess noise. Detector shot noise corresponds to the photon noise on the laser power incident on the detector (P_{D}). The noise power is proportional to $\sqrt{P_D}$ and has a white noise frequency spectrum. Detector thermal (Johnson) noise is the signal-independent noise of the detector and preamplifier and depends on the type of detector used. This noise also has a 'white' spectrum. Laser excess noise is the laser noise within the measurement bandwidth centered on the detection frequency. This noise is laser dependent and is influenced by mode competition and by optical feedback to the laser due to scattering from components in the optical system. It is found that the noise power spectrum shows an approximate $1/f$-behaviour. This 1/f-dependence is the reason that a high detection frequency is potentially a more sensitive technique than the lower frequencies usually applied in spectroscopic systems. The relative importance of these noise components depends on the detection frequency and on the laser power.

The wideband noise measurements discussed previously indicate, that there are regions at modulation frequencies beyond 100 MHz where the

1 /f-noise contribution can be neglected. Where shot noise dominates the system is called quantum noise *limited*. If we move the detection frequency range into such a potential quantum limited regime, 1 /f-noise contributions can be neglected and the total noise can be approximated as the sum of thermal and shot noise. Since the signal is proportional to P_D, shot noise to $\sqrt{P_D}$, and detector thermal noise is constant, it is clear that for high frequency modulation high laser-power gives improved SNR. If sufficient laser power is available on the detector, the power independent thermal noise does not contribute significantly to the total noise and shot noise remains the dominating contribution. The SNR under such quantum limited conditions is proportional to the square root of the laser power, P_D, available at the detector. For a typical laser we obtain $N \sim 3 \cdot 10^{15}$ photons. According to Poisson statistics we expect an ultimate lower detection limit of about $2 \cdot 10^{-8}$ for quantum limited conditions.

To complete the description of laser characterization, the far field pattern has been investigated with an infrared vidicon camera. It is obvious that the two filaments which can be observed in Fig. 2e are far away from a Gaussian beam profile and, therefore, it is difficult to transfer all optical power to the detector element. Especially for high frequency devices a small detector area is a main requirement. In the next section high frequency modulation schemes will be discussed and therefore the complex impedance of the laser measured with a high frequency network analyzer in the frequency range 50-200 MHz is shown in Fig. 2f. As is expected, the impedance is far away from the 50 Ω required for optimum radio frequency (rf)-power transfer to the laser in a 50 Ω-system and impedance has to be matched by a proper bias-T for high frequency modulation applications.

4. Sensitive detection techniques and applications

4.1. *High frequency modulation spectroscopy*

In the early 1980s, a spectroscopic method related to wavelength modulated or derivative spectroscopy-frequency modulation spectroscopy (FMS)-was developed [106–112]. In FMS, the laser is modulated at much higher frequencies than normally used in WMS, typically in the radio frequency (rf) region. In frequency space, the modulated laser electric field consists of a carrier frequency, which is the natural emission frequency of the diode laser, and sidebands displaced from the carrier by integral multiples of the modulation frequency. In the weak modulation limit, the laser spectrum can be approximated by a carrier with single upper and lower sidebands. When light within this spectrum is detected with a photodiode, each of the sidebands mixes with the carrier to generate a signal at the modulation frequency. In the ideal case, these two signals are equal in amplitude and 180" out of phase and, consequently cancel each other. If one of the sidebands is absorbed prior to detection, the balance condition between the sidebands is disturbed and a signal at the modulation frequency appears in the detector current proportional to the absorption. As the laser sideband is tuned through the absorption resonance, the amplitude of the rf signal duplicates the molecular absorption line shape. Although detection is usually performed at the modulation frequency, it can also be performed at various harmonics of the modulation frequency. Generally a coupling between amplitude and frequency modulation can be observed with semiconductor diode lasers. If carriers are injected periodically into the pn-junction of the laser, the carrier density (amplitude modulation) and the index of refraction (frequency modulation) in the laser resonator change with the injection current [113–117]. The degree of coupling of both modulations depends on the laser operating point and structure, and manifests itself as the so called residual amplitude modulation (RAM). Therefore, the theoretical description of FMS is conveniently expressed in terms of an electric field representation of the frequency and amplitude modulated laser radiation since this retains phase information [118,119]. When the laser drive current is modulated at ω_{rf} the laser output is both amplitude and frequency modulated and can be described by

$$E(t) = E_0\{1 + A4\sin(\omega_{rf}t + \Psi)\} \exp[i\omega_L t + i\beta\sin(\omega_{rf}t)] \quad (8)$$

where β and M are the frequency and amplitude modulation indices, Ψ is the phase shift between FM and AM (which for TDLs is typically about $\pi/2$), E_0 the electric field of the unmodulated laser. The term M represents the RAM of the laser. Eq. (8) can be rewritten using Bessel functions as

$$E,(t) = E_0 \sum_{n=-\infty}^{+\infty} r_n(\beta, M, \Psi)\, e^{i(\omega_L + n\omega_{rf})t}$$

$$r_n(\beta, M, \gamma) = J_n(\beta) + \frac{M}{2i} \times [J_{n-1}(\beta)\, e^{+i\Psi} - J_{n+1}(\beta)\, e^{-i\Psi}] \quad (9)$$

Pure amplitude modulation ($\beta = 0$) with $J_0(\beta = 0) = 1$ and $J_n(\beta = 0) = 0$ for $n = \pm 1, \pm 2, \pm 3, \ldots$ shows three frequency components in the laser beam at ω_L and $\omega_L \pm \omega_{rf}$. Pure frequency modulation (A4 = 0) leads to sideband coefficients $r_n = J_n(\beta)$ and a 180" phase shift for upper and lower sidebands with odd n. In the general case the intensities of upper and lower sidebands with equal order n differ in magnitude due to the superposition of AM and FM signals. The electrical field after the probe is $E_2(t) = E,(t)\ .T(\omega)$, where $T(\omega) = \exp\{-\delta(\omega) - i\phi(\omega)\}$ is the complex transmission function with absorption $\delta_n \equiv \delta(\omega_n)$ and dispersion $\phi_n \equiv \phi(\omega_n)$ of the sample. $T(\omega)$ interacts with the individual frequency components $\omega_n = \omega_L + n \cdot \omega_{rf}$ and we obtain

$$E_2(t) = E_0 \sum_{n=-\infty}^{+\infty} r_n(\beta, M, \gamma)\, e^{i(\omega_L + n\omega_{rf})t}\, e^{-\delta_n - i\phi_n} \quad (10)$$

The laser beam induces a photo current at the modulation frequency ω_{rf} at the square-law detector element, thus

$$i_{rf}(t) = i_0 \sum_{n,n'=-\infty}^{+\infty} r_n r_{n'}\, e^{i(n-n')\omega_{rf}t}\, e^{-\delta_n - \delta_n} \cdot e^{-i(\phi_n - \phi_{n'})} \quad (11)$$

If we account for the detector high frequency cut-off and apply a narrow band detection at the modulation frequency using a double balanced mixer, we can neglect the contributions proportional to $\exp(+im\omega_{rf}t)$ for $m > 1, 2, 3, 4, \ldots$. Therefore the indices n' are limited to $n' = n \pm 1$ and we obtain

$$i_{rf}(t) = i_0\{Z\, e^{i\omega_{rf}t} + \bar{Z}\, e^{-i\omega_{rf}t}\} \quad (12)$$

$$Z = \sum_{n=-\infty}^{+\infty} r_{n+1}\bar{r}_n\, e^{-\delta_{n+1} - \delta_n}\, e^{-i(\phi_{n+1} - \phi_n)} \quad (13)$$

If we define A = $2\mathrm{Re}(Z)$ and $D = -2\mathrm{Im}(Z)$ we obtain for the rf-current i_{rf}, the local oscillator signal i_{LO}, and the i_{IF} signal the output of the mixer

$$i_{rf}(t) = i_0\{A\cos(\omega_{rf}t) + D\sin(\omega_{rf}t)\} \quad (14)$$

$$i_{LO}(t) = i_{LO,0}\sin(\omega_{rf}t + \Theta) \quad (15)$$

$$i_{IF}(t) = \langle i_{rf}(t) i_{LO}(t)\rangle_\tau \quad (16)$$

where Θ is the phase shift. By inserting Eq. (14) and Eq. (15) into Eq. (16) we obtain after low pass filtering of sum frequency components at $(2\omega_{rf}t + \Theta)$ with a time constant τ as a detectable signal after the post mixer preamplifier

$$i_{IF} = Gi_0\{A(\beta, M, \Psi)\sin\Theta + D(\beta, M, \Psi)\cos\Theta\} \quad (17)$$

where G is the overall gain. Depending on the detection phase Θ, selectively the absorption ($\Theta = \pi/2$) or dispersion ($\Theta = 0$) of a spectral feature can be measured. With the above definitions for A, D, and Z and using $r_{n+1}\bar{r}_n = R_n + iI_n$ we can write for the general case for arbitrary AM-FM phaseshifts Ψ:

$$A = 2\sum_{n=-\infty}^{+\infty} \{R_n\cos(\phi_{n+1} - \phi_n) + I_n\sin(\phi_{n+1} - \phi_n)\}\, e^{-\delta_{n+1} - \delta_n}$$

$$D = -2\sum_{n=-\infty}^{+\infty} \{I_n\cos(\phi_{n+1} - \phi_n) - R_n\sin(\phi_{n+1} - \phi_n)\}\, e^{-\delta_{n+1} - \delta_n} \quad (18)$$

$$R_n = J_{n+1} J_n + \frac{M}{2} \{k_{1n} + k_{2n}\} \sin \Psi + \left(\frac{M}{2}\right)^2 \{k_{3n} - k_{4n} \cos(2\Psi)\}$$

$$I_n = \frac{M}{2} \{-k_{1n} + k_{2n}\} \cos \Psi + \left(\frac{M}{2}\right)^2 k_{5n} \sin(2\Psi) \tag{19}$$

$$\left.\begin{aligned} k_{1n} &= (J_n)^2 + (J_{n+1})^2 \\ k_{2n} &= J_{n-1} J_{n+1} + J_n J_{n+2} \\ k_{3n} &= J_n J_{n-1} + J_{n+1} J_{n+2} \\ k_{4n} &= J_{n-1} J_{n+2} + J_n J_{n+1} \\ k_{5n} &= J_{n-1} J_{n+2} - J_n J_{n+1} \end{aligned}\right\} J_v = J_v(\beta) \tag{20}$$

The formulas derived above are valid for all Ψ and M/β. There is experimental evidence that for semiconductor lasers at modulation frequencies around 100 MHz an AM-FM phaseshift of $\Psi = \pi/2$ can be expected [120]. In this special case the imaginary part I_n does not contribute and we obtain for the signal components:

$$A = 2 \sum_{n=-\infty}^{+\infty} \{J_{n+1}(\beta) J(\beta) + K_n(\beta, M)\} \cos(\phi_{n+1} - \phi_n)\, e^{-\delta_{n+1} - \delta_n} \tag{21}$$

$$D = 2 \sum_{n=-\infty}^{+\infty} \{J_{n+1}(\beta) J_n(\beta) + K_n(\beta, M)\} \sin(\phi_{n+1} - \phi_n)\, e^{-\delta_{n+1} - \delta_n} \tag{22}$$

$$K_n(\beta, M) = \frac{M}{2} \{k_{1n}(\beta) + k_{2n}(\beta)\} + \frac{M}{2}^2 \{k_{3n}(\beta) + k_{4n}(\beta)\} \tag{23}$$

where K_n describes the influence of residual amplitude modulation [112]. It is interesting to investigate this special case of $\Psi = \pi/2$ in the limit of low modulation ($\beta \ll 1$, $M \ll 1$) and additionally for low absorption and dispersion ($\delta_n, \phi_n \ll 1$). If we neglect higher order contributions as $M\beta, \beta^2$, M^2, we obtain $\sin(\phi_{n+1} - \phi_n) \approx \phi_{n+1} - \phi_n$ and $\cos(\phi_{n+1} - \phi_n) \approx 1$ and $\exp\{-\delta_{n+1} - \delta_n\} \approx 1 - \delta_{n+1} - \delta_n$. We can write $J_0(\beta) \approx 1$, $J_{+1}(\beta) \approx \pm \beta/2$, $J_n(\beta) \approx 0$, $|n| > 1$ for $\beta \ll 1$ and finally for the components A and D in this limit:

$$A \approx \beta\, (\delta_{-1} - \delta_1) + 2M = \beta\, \Delta\delta + 2M$$

$$D \approx \beta\, (\phi_1 + \phi_{-1} - 2\phi_0) = \beta\, \Delta\phi \tag{24}$$

For a β of unity and M/β of 8%, a typical absorption of 10^{-6} has an offset of about 0.16, which is several orders of magnitude higher than the desired absorption signal. In the absence of any absorption a background signal for the absorption proportional to M remains. For $M = 0$ this yields the formula derived by Bjorklund [107] for the detector current

$$i'_{rf}(t) = i_0 \{\beta\, A6 \cos(\omega_{rf} t) + \beta\, \Delta\phi \sin(\omega_{rf} t)\} \tag{25}$$

In the limit of low modulation and small absorption and dispersion, the absorption is proportional to the difference of absorption experienced by the upper and lower sideband. The dispersion signal D is proportional to the arithmetic mean of the phase differences between the upper (lower) sideband and the laser carrier. Both signals are directly proportional to the FM index β. In order to increase the signal amplitude one has to increase the modulation index and the optimum value for β is about 1.1. In the next section we will see that for higher values the signal amplitude decreases again. However, for these values of β the approximation is no longer valid and the explicit forms have to be applied. In the case of a simultaneous amplitude modulation, $M \neq 0$, the absorption signal has an offset proportional to $2M$, while the dispersion signal is offset free.

A third method of diode laser modulation spectroscopy is closely related to FMS: two-tone frequency modulation spectroscopy (TTFMS) [121–132]. This method offers the advantage that arbitrarily large modulation frequencies can be applied to the laser to maximize the differential absorption experienced by the sidebands, but detection at lower beat frequency allows the use of relatively low bandwidth detectors and demodulation circuitry. TTFMS is an attractive technique for monitoring absorptions that are pressure broadened to several gigahertz. It requires diode-laser modulation at two distinct radio frequencies ω_1 and ω_2 with detection at the difference between the two applied frequencies. (In the literature sometimes a different definition can be found [120,123,127]): center frequency ω_c and difference frequency Ω, with $\omega_1 = \omega_c + \Omega/2$, $\omega_2 = \omega_c - \Omega/2$.

The formal description is analogous to the single-tone case:

$$E_1(t) = E_0[1 + M_1 \sin(\omega_1 t + \Psi_1)][1 + M_2 \sin(\omega_2 t + \Psi_2)] \exp\{i[\omega_L t + \beta_1 \sin(\omega_1 t) + \beta_2 \sin(\omega_2 t)]\} \quad (26)$$

If we limit the discussion to slightly different modulation frequencies ($\omega_2 - \omega_1 = \Omega \leq 10$ MHz), we can assume $M_1 = M_2 = M, \Psi_1 = \Psi_2 = \Psi$, $\beta_1 = \beta_2 = \beta$. We can rewrite the expression for the electrical field:

$$E_2(t) = E_0 \sum_{n,m=-\infty}^{+\infty} r_n r_m \, e^{i(\omega_L + n\omega_1 + m\omega_2)t} \, e^{-\delta_{n,m} - i\phi_{n,m}} \quad (27)$$

$$\delta_{n,m} \equiv \delta(\omega_{n,m}), \qquad \phi_{n,m} \equiv \phi(\omega_{n,m})$$

$$\omega_{n,m} = \omega_L + n\omega_1 + m\omega_2 = \omega_L + (n+m)\,\omega_c + (n-m)\frac{\Omega}{2}$$

and obtain for the detector current:

$$i_{rf}(t) = i_0 \sum_{n,n',m,m'=-\infty}^{+\infty} r_n \overline{r_{n'}} r_m \overline{r_{m'}} \, e^{i(n-n')\omega_1 t} \, e^{i(m-m')\omega_2 t} \, e^{-\delta_{n,m} - \delta_{n',m'}} \, e^{-i(\phi_{n,m} - \phi_{n',m'})} \quad (28)$$

In contrast to the single-tone technique we detect the signals at the difference frequency ($n - n' = 1 \wedge m - m' = -1$) or ($n - n' = -1 \wedge m - m' = 1$). Therefore, the expression for the current simplifies

$$i_{rf}(t) = i_0 \left\{ e^{i\Omega t} \sum_{n,m=-\infty}^{+\infty} r_n \overline{r_{n-1}} r_m \overline{r_{m+1}} \, e^{-\delta_{n,m} - \delta_{n-1,m+1}} \, e^{-i(\phi_{n,m} - \phi_{n-1,m+1})} + e^{-i\Omega t} \sum_{n,m=-\infty}^{+\infty} r_n r_{n+1} r_m \overline{r_{m-1}} \, e^{-\delta_{n,m} - \delta_{n+1,m-1}} \, e^{-i(\phi_{n,m} - \phi_{n+1,m-1})} \right\} \quad (29)$$

It can be shown that both sums above are complex conjugate and finally we obtain as in the single-tone case absorption and dispersion elements. Only Eq. (13) has to be modified:32 + 13

$$Z = \sum_{n,m=-\infty}^{+\infty} r_n r_m \overline{r_{n-1}} \, \overline{r_{m+1}} \, e^{-\delta_{n,m} - \delta_{n-1,m+1} - i\phi_{n,m} + i\phi_{n-1,m+1}} \quad (30)$$

Some authors apply a further simplification [120]: under the assumption that the difference frequency is much smaller than the half-width at half maximum $\Gamma_{1/2}$ (HWHM) of the absorption line under investigation, the contribution to the dispersion signal disappears ($-i\phi_{n\,m} + i\phi_{n-1\,m+1} \approx 0$), while the absorption terms' add. The' expression for the detector signal is then:

$$i_{rf}(t) = i_0 \, 2\cos(\Omega t) \sum_{n,m=-\infty}^{+\infty} r_n \overline{r_{n-1}} r_m \overline{r_{m+1}} \, e^{-2\delta(\omega_L + (n+m)\omega_c)} \quad (31)$$

In this case the amplitude of the signal is no longer dependent on the difference frequency and the above equation describes the maximum possible amplitude for a minimum difference frequency. Furthermore, if β is so small that only first-order sidebands are significant, while Ω is small compared with the absorption linewidth and the differential absorptions $\delta_0 - \delta_{+1}, \delta_0 - \delta_{-1}$ and dispersions $\phi_0 - \phi_{+1}, \phi_0 - \phi_{-1}$ are small compared with unity, we obtain [129]

$$i_{rf}(t) = i_0[\beta^2(2\delta_0 - \delta_{+1} - \delta_{-1}) + 2M\beta(\delta_{-1} - \delta_{+1})\sin\Psi + M^2(2 - 2\delta_0 - \delta_{+1} - \delta_{-1})]\cos(\Omega t) \quad (32)$$

where the subscripts 0, + 1 and − 1 refer to sideband groups centered at frequencies $\omega_L, \omega_L + \omega_c + \Omega/2$ and $\omega_L - \omega_c - \Omega/2$. In the absence of any sample absorption, a background signal proportional to M^2 remains. This non-zero background carries with it the full amplitude noise spectrum of the diode laser and consequently limits the sensitivity of the technique. The main

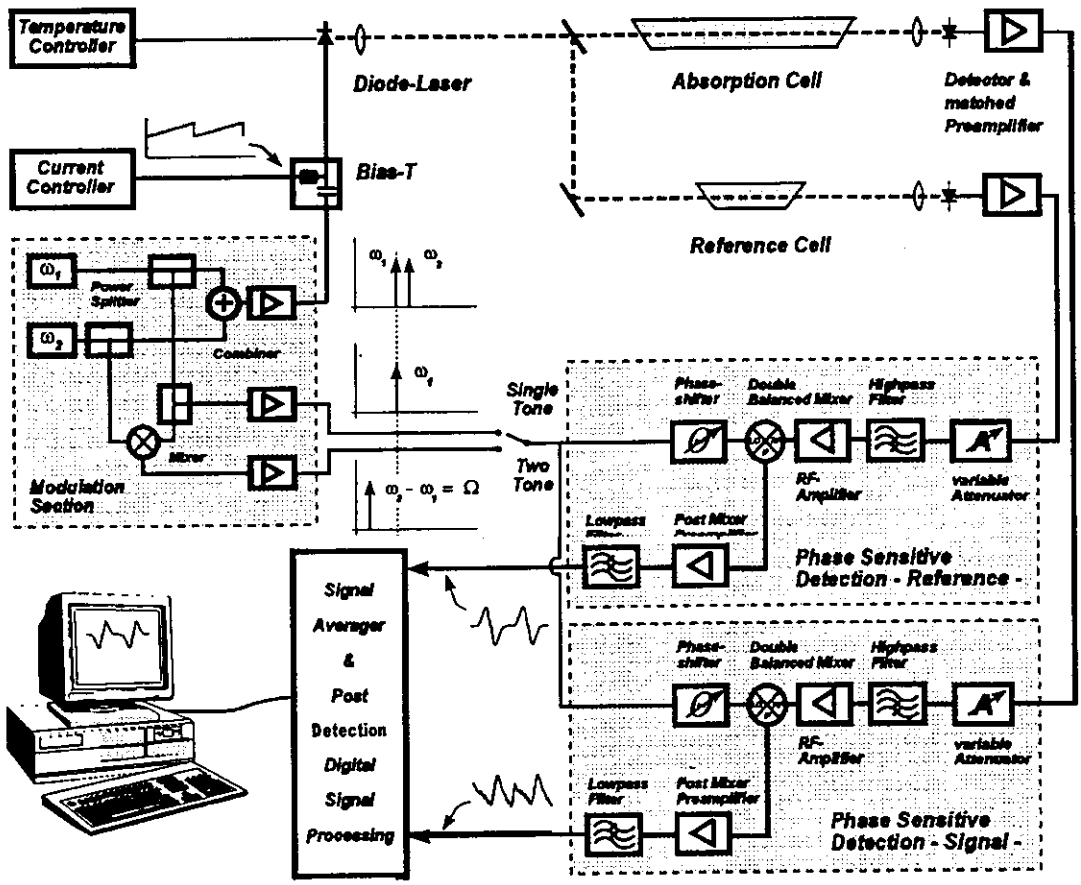

Fig. 3. Modulation/demodulation electronics, which allows to apply alternatively STFMS and TTFMS.

features of single-tone and two-tone spectroscopy will be summarized in the next section and specific advantages and disadvantages of both techniques will be discussed.

4.2. *Spectrometer operating conditions*

The principal differences between FMS and WMS are slight and the terms are somewhat misleading since in both cases it is the optical frequency of the laser that is modulated. They can be understood as the two limiting cases of the same technique. In FMS, the modulation index of the laser is small, but the ratio of the modulation frequency to the absorption linewidth is large; as a result the absorption feature of interest is probed by a single isolated sideband. In WMS the ratio of the modulation frequency to the absorption linewidth is small, but the modulation index is large. As a consequence, in WMS the absorption feature is probed with a large number of sidebands (comb structure). The experimental arrangement is essentially the same for both WMS and FMS and the optical systems based on White and Herriott cell designs in the mid- and near-infrared have already been discussed in Fig. 1. The laser frequency is modulated at ω_m by modulating the drive current. In the presence of an absorption line the frequency modulation of the' laser radiation produces an intensity modulation of the radiation transmitted through the cell and this is detected with a lock-in amplifier for WMS or a mixer for FMS. For high frequency modulation applications only bias-T's next to the lasers have

to be integrated and the detector bandwidth has to be adapted to the operating frequencies. Fig. 3 shows the principal layout of an electronic system designed for both single-tone and two-tone spectroscopy. The modulation section contains two independent rf-sources ω_1 and ω_2, which are combined in order to provide a two-tone modulation of the laser diode. If ω_2 is turned off, a single-tone modulation ω_1 can be attained. In contrast to other designs a passive combiner version has been chosen to avoid the generation of harmonic mixing products which can be encountered in designs based on the application of rf-mixers and frequency doublers. While in STFMS the single modulation frequency ω_1 is fed into the phase sensitive detection circuitry, for TTFMS a difference frequency $\omega_2 - \omega_1 = \Omega$ is generated by means of a rf-mixer. The phase sensitive detection device allows a phase shift to be introduced in the local oscillator (LO) branch. The sample and reference signals from the matched detector-preamplifier combination pass a variable attenuator and a highpass filter to prevent the rf-amplifier and the rf-input (RF) of a double balanced mixer from overloading. A low noise post-mixer-preamplifier and a lowpass filter following the intermediate frequency (IF) output of the mixer provide the sample and reference signals to a signal averager and further post-detection signal processing. Finally the data will be displayed and stored in a computer system.

For practical applications the parameters M/β and Ψ are determined by the available laser, while the modulation index β can be adjusted through the rf generator. The ratio of M/β is found to be approximately constant for a given laser and modulation frequency, and between 100 and 300 MHz values of typically 8% can be derived from the asymmetry of laser sidebands for lead-salt lasers. Since for high signals typical systems are operated at $\beta \approx 1$, the RAM offset will be one or two orders of magnitude less for TTFMS than for STFMS because RAM offset is proportional to M for STFMS and M^2 for TTFMS. On the other hand in STFMS an appropriate choice of the measurement phase will suppress the RAM offset while retaining the signal. Also the phase at which the RAM offset is eliminated depends on the relative phase Ψ of the amplitude and frequency modulation of the laser. For some lasers this phase can vary as the laser is tuned across the absorption line so that RAM suppression is not maintained across the line. The parameters ϕ and δ together with the linewidth can be varied through the cell pressure. Additionally the signal amplitude depends on the modulation frequency ω_{rf} in STFMS and ω_1 and ω_2 in TTFMS. The main challenge is to optimize the signal amplitude by proper adjustment of these operational parameters. A detailed description of lineshapes and their physical origin can be found in the literature [133]; here only the main features will be summarized. For the absorption δ and dispersion ϕ in the general case of a Voigt-profile we find:

$$\delta_V(\omega) = \delta_{Peak} V(x, Y) \tag{33}$$

$$\phi_V(\omega) = \delta_{Peak} L(x, Y) \tag{34}$$

with the VOIGT-function

$$V(x, y) = \frac{y}{\pi} \int_{-\infty}^{+\infty} \frac{\exp\{-t^2\}}{y^2 + (x-t)^2} \mathrm{d}t \tag{35}$$

and

$$L(x, y) = \frac{1}{\pi} \int_{-\infty}^{+\infty} \frac{(x-t)\exp\{-t_2\}}{y^2 + (x-t)^2} \tag{36}$$

where: $t = (\tilde{\nu}' - \tilde{\nu}_0)\sqrt{\ln 2}/\gamma_D$, $x = (\tilde{\nu} - \tilde{\nu}_0)\sqrt{\ln 2}/\gamma_D$, $Y = \gamma_L\sqrt{\ln 2}/\gamma_D$. Here γ_D and γ_L represent the Doppler and the Lorentz half width at half maximum (HWHM) of the absorption line; δ_{Peak} is Doppler-peak-absorption, $\tilde{\nu}$ the frequency and $\tilde{\nu}_0$ the frequency at line center. A number of techniques for calculating approximate values of the Voigt function are available [134]. The Voigt-linewidth γ_V can be approximated by [133]:

$$\gamma_V \approx 0.5346\gamma_L + \sqrt{0.2166(\gamma_L)^2 + (\gamma_D)^2} \tag{37}$$

Using the above expressions for ϕ and δ absorption and dispersion profiles as shown in Fig. 4a and 4b for a HO, absorption line in the ν_2-band at 1410.928 cm $^{-1}$ have been calculated based upon a concentration of 50 ppt at a pressure of 30 mbar and an optical absorption pathlength of 25 m. From the calculated Doppler- and Lorentz-width the Voigt linewidth has been estimated as 108.1 MHz. For simplicity we use in the

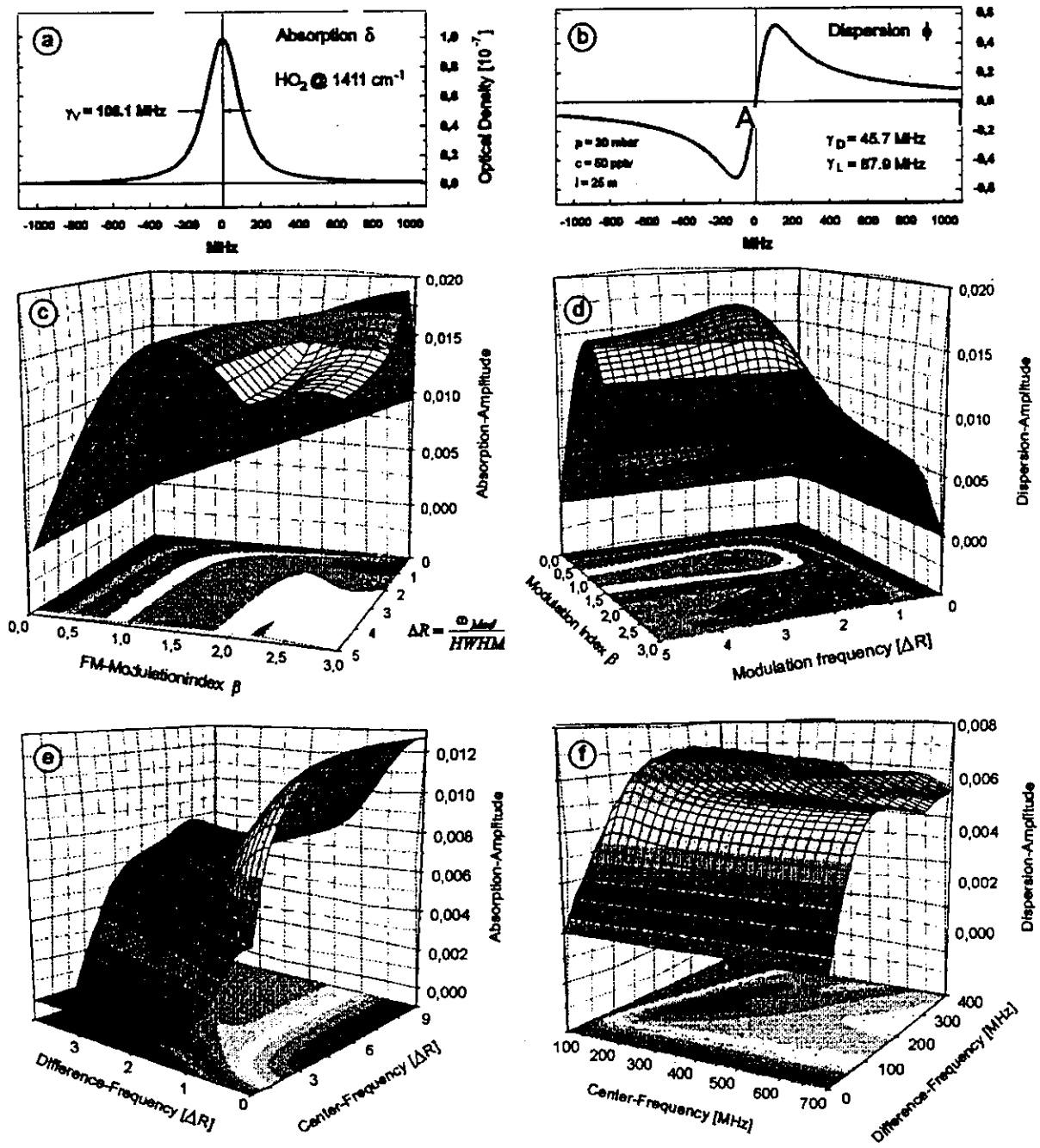

Fig. 4. Calculated absorption (a) and dispersion (b) signals for HO, based on a Voigt profile. STFMS peak amplitudes for absorption (c) and dispersion (d) and same calcualtions for TTFMS absorption (e) and dispersion (f).

subsequent example a value of 100 MHz. The combination of the line-profiles for ϕ and δ with the expressions for the STFMS and TTFMS signals detailed calculations of signal amplitudes under various conditions can be made. The most important features can be derived from the plots shown in Fig. 4. The calculations have been made under the assumption for $M/\beta = 0.08$, $\Psi = \pi/2$ and a peak absorption of 1% for STFMS (Fig. 4c, d) and TTFMS (Fig. 4e, f). The quantity AR = ω_{rf}/HWHM represents the ratio of the modulation frequency (STFMS) or center and difference frequency (TTFMS) to the half-width-at-half-maximum (HWHM) of the absorption line under investigation. The plots show the signal amplitudes as a function of modulation index β and modulation frequency ω_{rf} for STFMS and as a function of difference frequency and center frequency in terms of AR for a fixed modulation index $\beta = 1$. The single-tone (STFMS) signal has components both in-phase and in quadrature with the modulation. The in-phase signal is caused by absorption in the sample while the quadrature is due to dispersion in the sample and both can be used to measure species concentration. The absorption signal (Fig. 4c) reaches a higher amplitude than the dispersion signal (Fig. 4d) if low modulation frequencies and a high modulation index are applied ($\beta \gg 3$), which corresponds to WMS in the previously discussed sense. According to the strong M dependence of the signal offset and the associated RAM noise at low frequencies the absorption signal usually is not used for measurements. Optimum conditions can be observed for the dispersion signal as shown in Fig. 4d, when $\beta \approx 1.05$ and AR ≈ 2.2, which corresponds to a modulation frequency $\omega_{rf} \approx 2.2 \cdot$ HWHM. For a molecule with a HWHM at reduced pressure of about 100 MHz (e.g. HO,) this translates into an optimum modulation frequency of 220 MHz. For TTFMS the dispersion signal (Fig. 4f) requires a high difference frequency for highest signal amplitudes which leads to detection at frequencies comparable to the single-tone case. The calculated signal amplitude, however, is smaller by a factor of two and the advantage of low bandwidth detectors is not available. Therefore, only the absorption signal (Fig. 4e) is used for practical measurements. In contrast to single-tone the variation of the second modulation frequency has to be considered. A maximum signal amplitude can be found [120] for a modulation index $\beta \approx 1$. For this parameter the plot in Fig. 4f for the two-tone dispersion amplitude as a function of the difference-frequency and the center-frequency has been calculated and a maximum signal for $\omega_c > 5 \bullet$ HWHM and for $\Omega < 0.05 \bullet$ HWHM can be observed. As in the example above, for HO, this translates into a center frequency of 500 MHz and a difference frequency of 5 MHz; i.e. $\omega_1 = 505$ MHz and $\omega_2 = 495$ MHz.

Both techniques work with modulation frequencies in the white noise dominated high frequency region. However, STFMS detects the signals at the modulation frequency, ω_{rf}, while the two-tone scheme uses the difference frequency, $\Omega = \omega_2 - \omega_1$, of two discrete rf-signals. If laser noise is the limiting factor in the system, the two-tone beat frequency has to be chosen high enough to operate outside the 1/f-noise region in the shot noise dominated plateau. To enjoy the theoretically predicted sensitivity improvement, the two-tone technique has to use high frequency detectors as well, and the advantage of the use of cheaper detector elements is no longer valid. Therefore, modulation and detection at high frequencies in all types of FM instruments are recommended as long as there is no significant progress in manufacturing better single-mode diode lasers and laser excess noise at higher frequencies is significant. A lot of theoretical and experimental work has been done to evaluate both techniques. Each technique offers some unique advantages yet also has its drawbacks. The advantages of single-tone FMS are that simplest RF electronics can be used and the local oscillator phase can be adjusted to suppress the RAM signal. This technique can measure both absorption and dispersion of spectral features and as the signal occurs at high frequency usually above 100 MHz this technique is least sensitive to low frequency laser noise. On the other hand STFMS requires expensive, high-bandwidth and therefore small-area detectors. The technique is not suited to monitor pressure-broadened absorption lines with a HWHM in the Gigahertz range. If residual amplitude modulation cannot be suppressed efficiently, it limits the dynamic range. Two-tone

FMS can use large area detectors of moderate bandwidth (10 MHz), yield a flatter baseline and can monitor broad absorption features. However, it requires somewhat more complex RF electronics and is more susceptible to laser excess noise at the lower detection frequencies. Also there is no RAM suppression feature with local oscillator adjustment as in STFMS. Therefore, both modulation schemes should be implemented in new spectrometer designs as illustrated in Fig. 3 and then the optimum modulation scheme can be selected case by case. It seems that no definite decision can be made and the best method has to be selected depending upon the experimental conditions. The formalism derived so far will now be used to illustrate as an example the feasibility of the measurement of atmospheric HO,-radicals in the mid-infrared spectral region and it will be shown that there are other factors like background structures and nearby interfering lines that finally drive the decision for a special technique.

Based on this optimum parameter set for STFMS and TTFMS we will investigate in this section the feasibility of the measurement of HO, radicals in the atmosphere. For a modulation index of $\beta = 1.05$, a M/β ratio of 0.08 and a fixed AM-FM phase of $\Psi = \pi/2$ the spectral representations of STFMS and TTFMS are plotted in Fig. 5. The asymmetry of the sidebands cannot be seen on this scale. The first lower sideband in the single-tone case (Fig. 5a) at − 220 MHz has a phase opposite to the carrier indicated by (−). The amplitude of the sidebands at +_660 MHz has a contribution of only about 0.05% and at 880 MHz below 10^{-5}. For the two-tone case (Fig. 5b) the FM spectrum has been plotted for $\omega_1 = 600$ and $\omega_2 = 500$ MHz in order to separate the sidebands for the graphical representation, while for the calculation of the two-tone signals the previously discussed optimum values of $\omega_m = 500$ and $\Omega = 5$ MHz have been used. The signals for STFMS absorption (Fig. 5c), STFMS dispersion (Fig. 5e), TTFMS absorption (Fig. 5d) and TTFMS dispersion (Fig. 5f) have been calculated using the full formalism derived so far. The asymmetry in the signal amplitudes due to the simultaneous FM-AM modulation can clearly be seen. For clarity the seven orders of magnitude offset of the ST-absorption signal has been removed. For all line shapes as the modulation frequency is reduced the peaks move closer together, so that the in-phase single-tone signal resembles a first derivative lineshape and the two-tone quadrature signal resembles a second-derivative. From Fig. 5c–f we can understand what an 'isolated line' is: minimum and maximum of the dispersion signal lie within the HWHM of the absorption line under investigation and there is a contribution of maximum +_ 3 sidebands to the signal. That means that the signal amplitude remains unperturbed if within a range of + 7 linewidths (ca. 800 MHz) no other absorption-contributes to the signal. For strong interfering lines (water vapor) the separation has to be chosen even higher. So far the STFMS and TTFMS signals have been calculated for a set of optimum parameters for an isolated line. Now we will turn to a more realistic environment and investigate these signals and their interaction with background structures from nearby interfering lines in ambient air.

The band center of the fundamental bands of HO, are at 2.9 μm (ν_1), 7.2 (ν_2) and 9.1 μm (ν_3), with relative strength ν_2:ν_3:ν_1 = 3:1.8:1 [135]. There are electronic transitions at 1.25, 1.43 μm and a vi-overtone at 1.5 μm [136,137]. However there are a few pairs of lines in the ν_2-band overlapping within their Doppler width and the most suited can be found at 1410.928 cm^{-1} with line strength $S = 5.9 \cdot 10^{-20}$ cm $molec^{-1}$. A detailed search in the HITRAN database [138,139] at this preferable spectral region gives the following picture for spectral interference effects: CH, is the dominating interfering component near 1410.928 cm^{-1}, 600 MHz below and 5400 MHz above the HO, line center CH_4-absorptions might interfere, while at + 1.1 GHz a CO_2 line can be found. A water vapor absorption line at + 12 GHz offset from the HO_2 line center will lead to a slope superimposed to the FMS signal. The signals have been calculated for ambient mixing ratios (HO_2:10 ppt, H_2O:0.8%, CO_2:330 ppm, CH,: 1.8 ppm) for an absorption pathlength of 100 m at a pressure of 10 mbar. While the optimum conditions derived in the previous section for a pressure of 30 mbar were ω_{rf} = 220 MHz in the single-tone case and ω_m = 500 MHz/Ω = 5

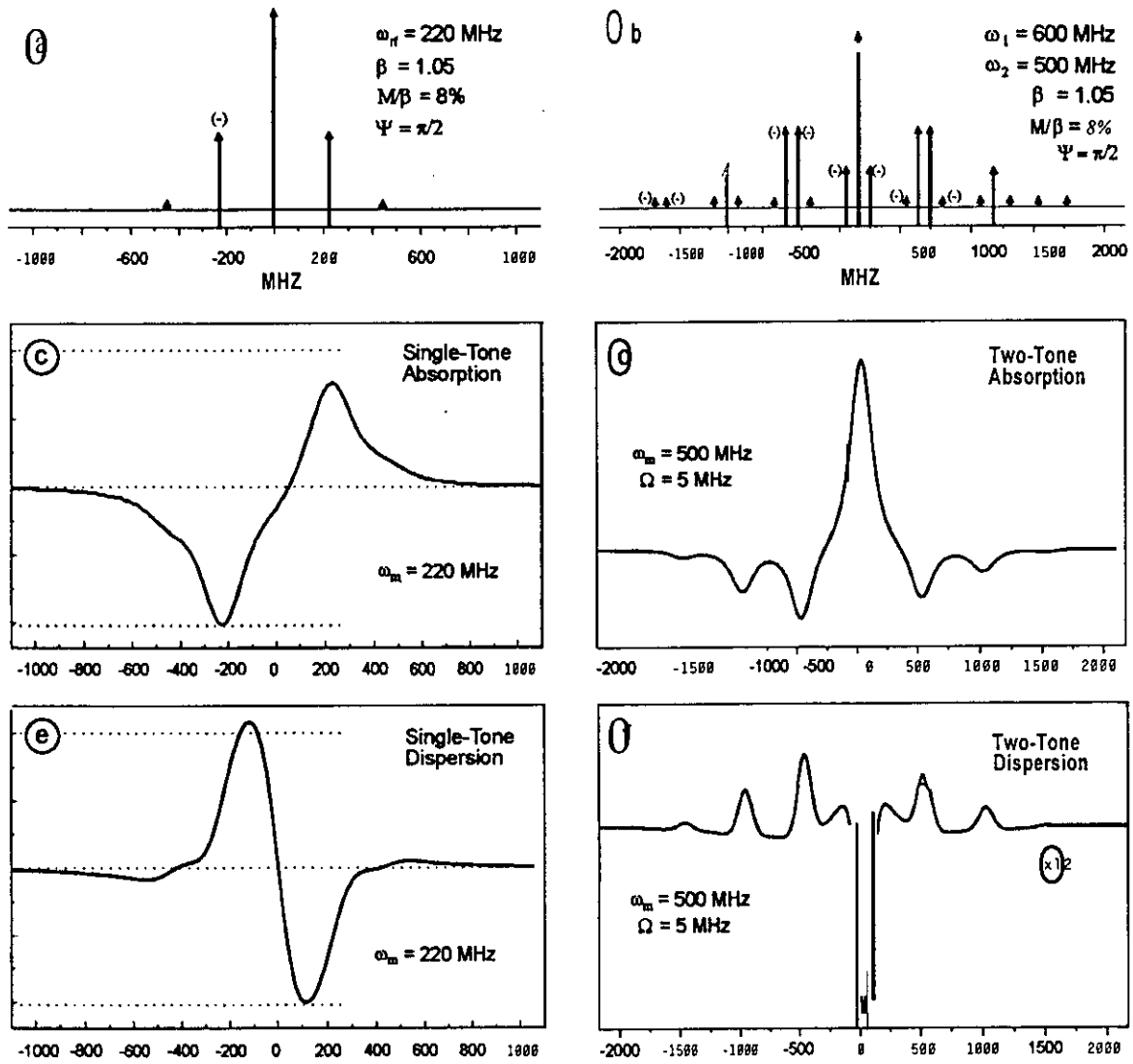

Fig. 5. Frequency domain representation of STFMS (a) and TTFMS (b) and calculated STFMS absorption (c) and dispersion (d) signals for a modulation frequency of 220 MHz. Same calculations for TTFMS absorption (e) and dispersion (f) signals for optimum modulation parameters.

MHz in the two-tone case, it can be seen that the modulation frequencies have to be chosen significantly smaller due to the interfering species in order to avoid strong mixing of signals. Therefore, for the final analysis a pressure of 10 Torr has been assumed giving an optimum modulation frequency of 120 MHz for STFMS. In Fig. 6 modulation frequencies of 60 MHz (a) and 120 MHz (c) have been used for the STFMS calculations and 100 MHz ±5 MHz (b) or 400 MHz ±5 MHz (d) for TTFMS calculations. The upper traces always show the pure HO_2 spectrum under the given conditions. Under these specific experimental conditions the more widespread two-tone HO_2 signals are more severely influenced by the CH, line nearby than the single-tone-signals are. At 1410.928 cm^{-1} a modulation frequency of about 60 MHz seems to be the best choice for

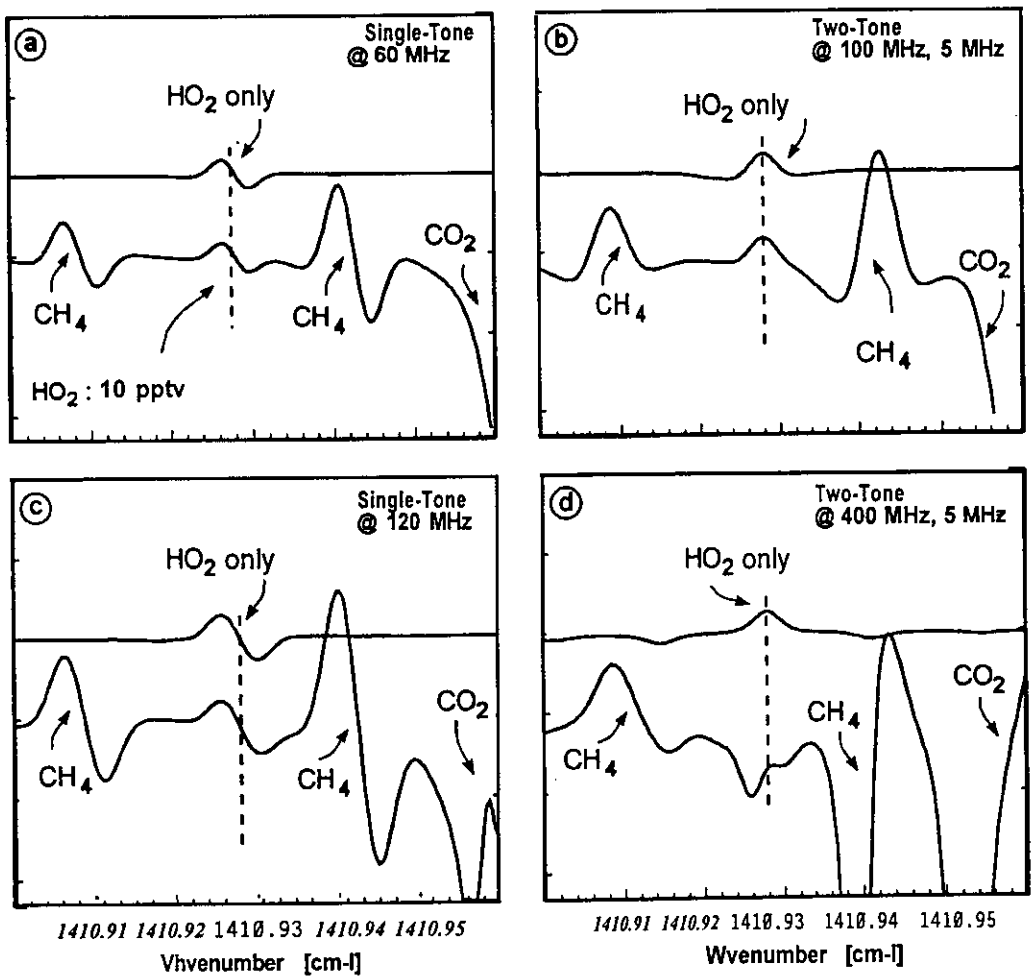

Fig. 6. Influence of interference from nearby spectral lines on the feasibility of HO, measurements near 1411 cm^{-1} for STFMS (a, c) and TTFMS (b, d).

long term signal averaging applications, where changes in the background structure of the signals deteriorate system performance. As a consequence, it is important to determine quantitatively interfering species or to remove them selectively from the sample gas. According to the instability of the HO,-radical the latter approach is not possible in this case. However, this is only a part of the complete discussion on HO, measurements and it was used to illustrate that besides principal specific advantages and disadvantages of the single-tone and the two-tone technique, the experimental conditions and requirements drive the final decision for the best technique.

The modulation techniques described so far have made it possible to detect absorptions below 10^{-6}. This sensitivity, when combined with an optical pathlength through an absorbing sample of several tens of meters, translates into parts-per-billion to parts-per-trillion detections for many molecular species in the infrared. To achieve these sensitivities, adequate for environmental monitoring, absorption spectrometers require multi-reflection optical systems. In all these systems, the sensitivity gained by lengthening the absorption path is increasingly offset by the attenuation of the radiation power throughput, due to the increasing number of reflections and the imperfect

reflectivity of the mirrors. Consequently, each absorption spectrometer has to be operated with an optimal number of reflections in multi-reflection absorption systems to achieve the best SNR [140]. At conditions usually encountered in tunable diode laser spectrometers, the optimal number of passes for the FM spectrometers has been found to be much smaller than the optimal number of passes for the spectrometers using the conventional derivative technique. This finding implies that, if both techniques are operated with an optimal number of passes, the introduction of FM techniques can improve the ultimate SNR in spectrometers using optical multipass cells by only about an order of magnitude. Although still highly desirable,' this is substantially lower than the two orders of magnitude potential improvement derived solely from the noise analysis, without considering the use of multipass cells and to overcome this limitation higher laser power and/or a higher cell transmission is required.

A selection of molecular species that can be detected using near-IR and lead-salt diode lasers is listed in Table 1. Also shown is the detection limit in terms of volume mixing ratio [pptv] and [μg m^{-3}] assuming an absorbance sensitivity of 10^{-6} @ $\Delta f = 1$ Hz and a 25 m optical path-length. The absorption lines listed are not necessarily the strongest for that species nor do the wavelengths λ necessarily represent the only regions in which the species can be monitored. The detection limits must be regarded as estimates only and much depends on instrumental factors such as the quality and availability of the laser. By averaging over periods longer than 1 s or by using longer path-lengths the detection limits can be improved. While the predicted sensitivities are based on known line strengths and the optical performance of a typical TDLAS system, it is in the nature of field measurements that optimum instrumental performance is not always achieved. In comparing the sensitivities achievable experimentally with the different modulation schemes, it is important to distinguish between carefully controlled laboratory experiments using short optical paths, and TDLAS measurements. It is also necessary to precisely define the meaning of sensitivity and detection bandwidth or integration time.

A broad range of investigations and applications of FM spectroscopy has been reported [141-166]. Carlisle et al. [128] have reported quantum limited performance with a sensitivity of $5 \cdot 10^{-8}$ using TTFMS at 1 Hz bandwidth, a 200 mm cell and a laser with a power of 640 μW. Werle et al. [118] have demonstrated a sensitivity of $2.5 \cdot 10^{-6}$ for STFMS at a bandwidth of 1.56 kHz using a 1450 μW lead-salt diode laser. This translates into a sensitivity of $6 \cdot 10^{-8}$ at a 1 Hz bandwidth assuming the theoretical dependence of noise on bandwidth. Silver has .given a theoretical comparison of the various modulation techniques [127] using typical values for the laser parameters, and in a companion paper Bomse et al. [141] compare the sensitivities achieved experimentally using the same laser in different modulation schemes. They used a 110 mm cell and piezo-electrically vibrated the beam steering mirrors as a means of suppressing the optical fringes. Silver's theoretical predictions are that the intermediate frequency techniques, with modulation between 100 kHz and 10 MHz and detection either at the modulation frequency ω_m or at $2\omega_m$ should perform as well as either STFMS or TTFMS. This is confirmed by the experimental findings, although these must be tempered by the fact that a rather low-power laser (11 μW incident on the detector) was used and that the STFMS experiments did not achieve optimum results because of detector problems. The best sensitivity of $2.5 \cdot 10^{-6}$ was achieved with a detection frequency of 10 MHz and a modulation frequency of either 10 or 5 MHz (second harmonic). In both cases the measurement was detector-noise limited so a more powerful laser would have improved the sensitivity. A similar comparison of WMS, higher frequency WMS and TTFMS modulation schemes has been carried out by Pavone and Inguscio for a GaAlAs laser at 886 nm [130]. They found sensitivities of $4.5 \cdot 10^{-7}$, $9.7 \cdot 10^{-8}$, and $6.4 \cdot 10^{-8}$, respectively, for the three techniques, broadly in line with the results of Bomse et al. [141] for lead-salt lasers. A series of laboratory investigations, feasibility studies and even field applications have been performed with FM spectrometers. Johnson et al. have applied TTFMS for high sensitivity detection of water

Table 1
Calculated TDLAS detection limits for selected molecules for a detectable optical density $d\Omega^{-6}$ @ $\Delta f = 1$ Hz, a pressure of 30 mbar (150 mbar for $\lambda < 2.7$ μm) and 25 m optical pathlength

Gas	Wavelength λ		Linestrength S	Detection limit	
	(cm-^{1})	(μm)	(cm mol^{-1})	(pptv)	(μg m^{-3})
H_2O	7323.945	1.365	$6.599 \cdot 10^{-21}$	900	0.73
	1684.835	5.935	$2.919.10^{-19}$	23	0.02
HF	7855.643	1.273	$7.591 \cdot 10^{-20}$	71	0.064
	7515.803	1.331	$1.34 \cdot 10^{-20}$	290	0.25
C_2H_2	3260.427	3.067	$2.29 \cdot 10^{-19}$	33	0.038
CH_3Cl	3040.220	3.289	$1.92 \cdot 10^{-21}$	$3.1 \cdot 10^{"}$	7.1
CH_4	3067.300	3.260	$2.129.10^{-19}$	36	0.026
	6057.086	1.651	$1.28 \cdot 10^{-21}$	$3.6.10^{3}$	2.6
HCl	2944.914	3.396	$5.033 \cdot 10^{-21}$	12	0.02
	5723.301	1.747	$1.179 \cdot 10^{-20}$	360	0.58
H_2CO	278 1.035	3.596	$5.93 \cdot 10^{-20}$	130	0.17
HBr	2649.092	3.775	$4.456.10^{-20}$	96	0.35
	7458.082	1.341	$2.073 \cdot 10^{-23}$	$217 \cdot 10^{3}$	785
HI	2277.519	4.391	$2.08 \cdot 10^{-21}$	$1.6 \cdot 10^{3}$	55
CO_2	2270.290	4.405	$3.358 \cdot 10^{-20}$	160	0.31
	4989.972	2.004	$1.332.10^{-21}$	$3.1 \cdot 10^{"}$	6.1
	6240.105	1.603	$1.838 \cdot 10^{-23}$	$235 \cdot 10^{3}$	6.1
N_2O	2236.224	4.472	$1.004 \cdot 10^{-18}$	5	0.01
	5117.472	1.954	$5.11 \cdot 10^{-23}$	$81 \cdot 10^{3}$	159
c o	2169.198	4.610	$4.615 \cdot 10^{-19}$	11	0.014
	6330.167	1.580	$1.59.10^{-23}$	267.10'	333
o c s	2052.716	4.872	$1.03 \cdot 10^{-18}$	5	0.015
NO	1875.813	5.331	$3.399 \cdot 10^{-20}$	140	0.19
HNO_3	1722.372	5.806	$7.2.10^{-20}$	87	0.24
NO_2	1600.413	6.248	$2.18 \cdot 10^{-19}$	20	0.042
	12500	0.800	$5 \cdot 10^{-23}$	105.10"	215
HO_2	1411.182	7.086	$1.2.10^{-20}$	450	0.66
SO_2	1371.695	7.290	$4.855 \cdot 10^{-20}$	130	0.38
H_2S	1364.601	7.328	$1.02.10^{-21}$	$8.0 \cdot 10^{3}$	12
H_2O_2	1284.205	7.787	$4.464.10^{-20}$	130	0.2
HCOOH	1113.068	8.984	$4.4.10^{-20}$	130	0.26
O_3	1052.848	9.498	$4.2.10^{-20}$	100	0.22
O_2	7880.637	1.269	$6.229.10^{-26}$	$64 \cdot 10^{6}$	$92 \cdot 10^{3}$
	13142.57	0.761	$7.71.10^{-24}$	$674 \cdot 10^{3}$	963
NH,	930.757	10.744	$5.2 \cdot 10^{-19}$	9	0.007
	6478	1.544	$3.7.10^{-22}$	$12 \cdot 10^{3}$	9.2

vapor and the measurement of the line-strength in the HO, ν_1 overtone band at 1.5 μm using an InGaAsP laser [142–144]. A series of applications with focus to water vapor measurements has been reported [145–149]. In the field of medical diagnostics Cooper et al. have reported on measurement of $^{12}CO_2/^{13}CO_2$ ratios with a 1.6 μm distributed feedback semiconductor diode laser [150]. In order to investigate samples from arctic ice cores Güllük et al. have successfully applied a high frequency modulated TDLAS for measurements of CO,, CH,, N_2O and CO in air samples of a few cm^3 based on mid-infrared lead-salt diode lasers [151]. Mücke et al. investigated the feasibility of HO, measurements in the mid-infrared near 1410 cm $^{-1}$ and in the near-infrared for the v,-overtone at 1.5 pm by using single-tone and two-tone FMS [152]. They also investigated

in detail the calibration procedures for such systems [153] and in a series of intercomparison studies the application of TDLAS for QA/QC studies with focus on the validation of formaldehyde measurement techniques [154,155]. In a joint action between the Fraunhofer Institute in Garmisch-Partenkirchen and the Max Planck Institute in Mainz, two different FM spectrometers and other chemical sensors have been applied to an intercomparison of formaldehyde measurements [156]. Meanwhile there is evidence on the performance of the high frequency modulation schemes in field-capable TDLAS instruments. Wienhold et al. used a fast TTFMS system for trace gas flux measurements [38,157]. Werle et al. [35,158] have reported field measurements using a single-tone FMS system and a modified version has meanwhile been successfully used for trace gas flux measurements by the eddy correlation technique [159]. Some work has been reported on the investigation of multicomponent TDLAS applications [160-162]. However especially in the near infrared an increasing number of applications is to be found [163-165].

To put the following discussion in context we note that for NO_2, a species of average linestrength, an absorbance of 10^{-5} corresponds to 50 pptv, assuming use of the strongest NO, absorption line at 1600 cm^{-1} and a path-length of 100 m. Under controlled laboratory conditions, absorption sensitivities of around 10^{-6} are achievable for WMS systems. However for TDLAS field measurements 10^{-5} is considered a good performance. This sensitivity can be improved to about $3 \cdot 10^{-6}$ by averaging over 60 s. Provided that drift problems can be avoided by taking regular background spectra, this figure can be improved further by even longer averaging periods. Assessing the potential performance of the higher frequency modulation schemes is more difficult firstly because the sensitivity is much more dependent than with WMS on laser parameters, such as the laser power, noise spectrum and amplitude modulation index. Also the laser beam quality is important since the radiation must be focused onto a small-area-detector, which is needed to give larger bandwidth. Secondly, the sensitivity can be limited by fringes or other experimental artefacts such as thermal drifts. Because of these factors, any reported sensitivity obtained using a particular modulation scheme normally applies only to the specific laser and experimental arrangement used to produce it. Consequently, general statements about superiority of one of the modulation techniques are hardly possible.

4.3. *Optical fringes and sample modulation enhanced FM-spectroscopy*

In most sensitive instruments, the diode laser is repetitively tuned over a molecular absorption line and the spectra are averaged over a specified time interval. When the wavelength of the diode laser is tuned over an absorption line, a periodic fringe structure is superimposed to the desired signal from the absorption of the target gas ('etalon-effect'). If this fringe structure is generated between the reflecting mirrors in the multipass absorption cell, thermally induced mechanical drifts cause a change of the fringe structure, which usually limit sensitivity due to their variation with time. The uncertainty due to these fringes is not bandwidth dependent, whereas random noise components decrease as $\sqrt{\Delta f}$. At longer integration times reduction in random noise often results in little overall improvement since the measurement uncertainty becomes limited by the optical fringes. For all spectroscopic techniques the problem of fringe reduction remains the main challenge in order to improve sensitivity. In general, fringe reduction techniques can be categorized in techniques applying mechanical modulation or dithering of the etalon spacing, modified modulation schemes, background subtraction and post-detection signal processing. If the etalon path-difference is mechanically modulated then the fringes will shift relative to the absorption spectrum. As the spectrum is averaged the fringes will then average to zero, provided the modulation amplitude corresponds either to an integral or a large number of fringes. One method of accomplishing this modulation has been demonstrated by Webster [166] who interposed an oscillating Brewster plate into the beam at a point between the two surfaces

forming the etalon. Oscillating the plate by typically 1" varies the optical path-length through the plate. Because the plate is at the Brewster angle reflection losses are minimised. One disadvantage of this method is that it is difficult to apply to a multipass cell without causing significant attenuation of the beam. Silver and Stanton [167] suggested an alternative method using a piezoelectric transducer to vibrate the mirror or another component which forms one surface of the etalon. They successfully applied this technique to a Herriott cell in which they vibrated one of the spherical mirrors. Both techniques are difficult to implement in a complex TDLAS system where many optical surfaces may cause etalons. Cassidy and Reid [168] have shown that in TDLAS systems using WMS the fringes can be averaged to zero by applying an additional low-frequency wavelength modulation to the diode laser, with an amplitude equal to an integral number of periods of the etalon. This is similar in effect to the modulation of the etalon pathlength described above except that the absorption spectrum is also shifted by the wavelength modulation. As a result the technique is effective only at removing fringes with a period less than the absorption linewidth since the modulation amplitude needed to remove longer period fringes would also smear the absorption lineshape and reduce its peak height. Sun and Whittaker [169] have considered the application of this technique to FMS systems and show that in this case longer period fringes can be effectively reduced. Post-detection signal processing can take the form either of analogue processing of the signal from the lock-in amplifier or demodulator, or digital processing of the signal acquired by the signal averager. Both take advantage of the periodic nature of the optical fringes. A simple low-pass filter following the phase sensitive detection can dramatically reduce fine-pitch fringes [118,128].

While many improvements in modern TDLAS systems focus on optimizing optical components, much less effort has been put into post detection signal processing [170-174]. In operational TDLAS systems, a combination of background subtraction with some form of post detection processing is most commonly used. Trace gas measurements near to the detection limit are usually performed by measuring alternatively the spectrum of the ambient air and air devoid of the target substance, which we refer to as a background spectrum. This procedure is based on the inherent assumption that within the time interval needed for the acquisition of both spectra the background structures do not change. If this assumption is fulfilled, the substraction of the background spectrum from the ambient spectrum would provide the absorption spectrum of the target species which, to a first approximation, is only subject to random noise. After the subtraction of background structures, the ambient spectrum is fitted to a calibration spectrum, obtained when the absorption cell is filled with a stable calibration gas mixture. From time to time such a spectrum is recorded and stored for signal processing. A signal processing concept for TDLAS must provide means for correcting frequency and amplitude fluctuations as well as having some capability to cope with changing background structures. Therefore, an intensity normalization process is required to correct for amplitude variations and to determine the concentration values from ambient spectra. In most spectroscopic measurements the detected signal is proportional to the trace gas concentration and depends on the laser power. Intensity fluctuations of the laser or changes in the optical system alignment can generate a variation in the reported concentration data, which is not real. Therefore, an intensity normalization has to be applied to measured data. The conventional approach to measure laser intensity I_0 is to couple out a certain amount of energy from the main beam using a beam splitter and monitor the laser power drift with a reference detector. A more direct method is to monitor the average detector current, which is (after dark current subtraction) proportional to the number of photons incident upon the detector. The deviation in the detector bias can be attributed rather to changes in the background radiation as for example sunset, sunrise or clouds passing by during the measurements rather than to changes in laser intensity or alignment. Therefore, a novel concept for an improved intensity normalization is based on the measurement of the average rf-

modulation signal amplitude [172]. For frequency modulated semiconductor lasers there will always be a residual rf-current at the modulation frequency, which is proportional to the laser power incident upon the detector and accounts for changes in the laser intensity as well as for changes in the optical system alignment. A fraction of this current can be used for normalization techniques, which leads to a significant improvement in system stability. In contrast to the conventional techniques, the rf-normalization is insensitive to changes in the background radiation and for high frequency modulation techniques, the rf-power level at the detector ideally represents variations in laser power and system alignment changes.

The discussion of optical fringes has shown that broad fringes can appear as a linear slope superimposed on the desired TDLAS signal. The linear regression scheme conventionally used can yield incorrect results when the signal is distorted, which is especially critical at low ambient concentrations [172]. Depending on the direction of the slope of the background, the linear regression tends to over- or underestimate the concentration of the ambient gas. Much more critical is the impact of drifts on the ambient spectra relative to the calibration spectrum. These drift effects can lead to a significant underestimation of the monitored gas concentration, i.e. a spectrometer can report extremely low concentration values and possible variations in the calculated data could refer to drift effects rather than the changes in ambient trace gas concentrations. While the sensitivity towards drift is the same for symmetric signals (2nd derivative, TTFMS) and for asymmetric signals (1st derivative, STFMS), it can be shown that symmetric signals are less susceptible to changes in the slope of the background. Variations in the laser current due to noise and other interfering signals have a dramatic influence on the system performance, especially on the confidence range of the measurement and therefore on the detection limit of the system. An order of magnitude in performance can easily be gained or lost, depending on the stability of the laser and a signal averager is required for a signal-to-noise ratio improvement together with an online correction of frequency fluctuations in the ambient spectra.

The application of modern signal processing is a promising concept and might help to improve precision and accuracy in tunable diode laser spectroscopy. Although a potential a priori control structure and some performance criteria can be defined, it is generally not possible to specify, in advance, the parameters within this structure. This situation calls for the introduction of adaptivity. The essential and principal property of an adaptive system is its time-varying, self-adjusting performance by continually seeking the optimum within an allowed class of possibilities, which would give superior performance compared with a system of fixed design. A promising approach is the use of a multiple linear regression scheme. The multiple linear regression (MLR) is an extension of the conventionally used linear regression scheme and offers more degrees of freedom for the fit process. While the linear regression uses only information about the background and the structure of the calibration signal, the multiple linear regression scheme allows more parameters to be added. A slowly moving fringe structure generates a time-varying background structure which calls for adaptive signal processing in the previously discussed sense. An adaptive control structure which has proven to be extremely useful is the adaptive Wiener filter. The purpose of an optimal filter is to recover the desired signal from the actually recorded signal. While the multiple linear regression scheme has no time delays, the Wiener filter is able to detect signal drifts and therefore has a 'shift correction option' as an integral part. The most exciting feature of the adaptive filter is that, in principle, no background spectrum is required and therefore background spectra could probably be omitted, which also would improve the duty cycle of the measurement. Current work in TDLAS development is focused on the implementation of online, adaptive Wiener [172] and Kalman filters [171] to improve system performance. The adaptive Wiener filter uses a minimum mean square error algorithm (MMSE) to determine the optimum set of filter coefficients for a finite impulse response (FIR) filter. For each ambient spectrum a calculation of

the filter coefficients is performed and therefore the filter is able to adapt to changing conditions such as signal drift and changing background structures. Averaging of these filtered spectra should then improve the detection limit according to a square root relationship. This has been tried but the achieved improvement was always substantially smaller than that expected on the basis of the square root relationship for signal averaging. The observed deviations are most probably caused by the violation of the assumption of stationarity caused by drifts in the system such as temperature changes, moving fringes or background changes [175,176]. Therefore, care must be taken with appropriate averaging times when determining time averages, and we have to ensure stationarity during the averaging interval. Stationarity implies that statistical quantities such as the mean and variance, do not vary with time. For example, if we find the mean concentration of a stable calibration gas at t_0, it should be identical with the value found at t_0 + At. Unfortunately, we do not have at our disposal an ensemble of identical experimental setups, which may be used for simultaneous experiments. Usually, we have a single function of time, say, of trace gas concentrations, and we must assume ergodicity to obtain estimates of ensemble averages. An ergodic random process is one whose infinite time average is equal to its ensemble average and, if we can make this assumption, then we can substitute time averages wherever we have ensemble averages. This leads to another problem. We cannot average forever as required in the ergodic hypothesis. Our only hope is that the process is sufficiently band limited so that a reasonable averaging time will give a stable result. For a perfectly stable system, a background spectrum obtained by supplying zero air to the instrument inlet, would display the same etalon fringes as the sample spectrum. Subtraction of this background spectrum would then remove the fringes. However, real systems are subject to thermal drift, so that in the time between taking the sample spectrum and the background spectrum the fringes will have drifted and cancellation will not be perfect. Thus the background subtraction is more successful the more stable the system is and the more rapid sample and background measurements can be alternated. The instrument stability can be characterized using the Allan variance [175]. As long as white noise dominates the system, the Allan variance is equivalent to the conventional variance and can be used to predict the detection limit of a given system as a function of the integration time. A plot of the Allan variance as a function of the integration time usually shows a minimum, which corresponds to the optimum integration time, typically on the order of 40- 100 s. This finding has been confirmed by many other researchers working in the field of TDLAS [34]. The optimum integration time is a characteristic property for a given instrument as it reflects the overall stability and, therefore, can be used to predict the system performance.

Recently it has been shown that signal fluctuations at low optical densities caused by interferometric effects [99,177,178] might give an explanation for the fact, that the expected improvement in system performance after the application of high frequency modulation schemes to spectroscopic systems designed for conventional derivative spectroscopy has not yet been attained on a routine bases. When measuring weak absorption and dispersions one should keep in mind that for phase sensitive detection techniques fluctuations in the optical pathlength have to be considered. Especially problems associated with the propagation of laser beams through turbulent flows in optical multipass cells, where very small changes in the refractive index are present have to be considered. These small changes in refractive index are related primarily to the small local variations in temperature and pressure, which are produced by the turbulent motion of the sample gas, when the air is expanded from atmospheric pressure into the flow pressure regime of the multipass cell, which is typically operated at a reduced pressure. While the refractive index variation from the mean value is very small, in a typical situation of practical interest a laser beam propagates through a large number of refractive index inhomogeneities, and hence the cumulative effect can be very significant and produce optical phase effects, which in turn lead to angle-of-arrival fluctuations or beam wander, intensity fluc-

tuations, and beam broadening. As an aid in understanding the effects of the refractive index fluctuations, a region of high or low refractive index can be thought of as an eddy, which may behave similar to a lens. In this model the cell-atmosphere may be thought of as a large number of random lenses, having different shapes and scale sizes, that move randomly through space. A limited system stability has been observed by many researchers, who use quite different system designs, but similar cell pressure, gas flow and mechanical, optical and electronical components, with respect to temperature coefficients, for example. While temperature effects seem to dominate when we investigate drift effects, short term fluctuations might be caused by a turbulent gas flow in the commonly used optical multipass cells. There are actually three ways in which pressure fluctuations can degrade diode laser spectrometer performance. The first one relates to the effect that refractive index-induced phase fluctuations affect the measurement in sensitive phase detection schemes. In this context, pressure fluctuations are shown to cause a change in phase between the carrier and sideband wavelengths. These fluctuations then result in voltage fluctuations out of the phase sensitive detector which is set for constant phase. The second effect relates to the fact that pressure changes in the cell directly result in optical changes and the third effect results from various spatial imaging fluctuations on the detector. It turns out that turbulence effects severely affect FM-spectrometers, which have the potential to reach the quantum limit. However, turbulence effects might also be important for conventional, derivative or direct absorption spectrometers and we are not aware of any investigation on the effect of turbulence in multipass cells on beam wander, angle-of-arrival fluctuations, intensity fluctuations and beam broadening. Modern multipass cell designs already utilize an improved gas flow, in order to obtain a laminar flow for fast exchange times and, therefore, we expect such a Herriott type cell to be superior for ultrasensitive measurements at low optical densities. In conclusion, similar limits of detection in optical multipass systems suggest a significant contribution of turbulent refractive index fluctuations to the detection limit of state-of-the-art FM-spectrometers using atmospheric open paths and optical multipass cells and this effect has to be considered for systems, designed for near quantum limited applications.

We will now return to the fringe problem and slow fluctuations due to thermal drifts. All fringe reduction techniques have the same drawback, that they operate only for a special type of background structure and an effective suppression of all accidental etalons could, in principle, only be obtained by a combination of several of these techniques. However, it has been found in most practical applications that the combined effect of different suppression schemes is not as efficient as the sum of the individual effects. An effective fringe reduction technique requires selective modulation of the sample spectral feature under investigation without affecting fringes and background structure. This modulation has to be faster than the optimum time constant derived from the Allan variance analysis. A basic approach is the background subtraction technique described previously. Another promising approach is the use of an additional sample modulation to separate disturbing background effects from the molecular feature of interest. Examples for such a sample-modulation enhanced FM-spectroscopy are photochemical modulation [179], magnetic rotation spectroscopy (MRS) [180-182] and Stark-modulation [176]. In order to provide an additional sample modulation available for a multitude of molecules we applied the Stark-effect, because important molecules as ammonia, nitric acid, formaldehyde, hydrogen peroxide, hydrogen fluoride and many others show a permanent electric dipole moment, which is a prerequisite for interaction with an external electric field. The sample modulation approach is an extension of the high frequency modulation technique.

The basic element of the extra setup for a double modulation includes a special sample modulation cell, which has been designed to generate a strong electric field perpendicular to the laser beam for Stark modulation [183]. Additionally a second phase sensitive detection device, usually a lock-in amplifier, has to follow the FM electronics output. The laser-sample double mod-

ulation technique has been applied to formaldehyde (HCHO), which is well suited due to its strong electric dipole moment of 2.34 Debye. A doublet ($5_{32}-4_{31}$ and $5_{33}-4_{33}$) at 1757.94 cm^{-1} with a line strength of $4.1 \cdot 10^{-20}$ cm $molec^{-1}$ showed a suitable Stark-splitting. For this experiment a sinusoidal AC-high voltage has been applied to the electrodes of the Stark absorption cell, whereas the same modulation signal was fed at the same time to the reference input of the lock in amplifier, which has been used for phase sensitive detection of the Stark modulated signal provided at the post-mixer-preamplifier output. For the purpose of an intercomparison between the conventional FM technique and this FM-Stark double modulation technique, time series data obtained from the measurement of a constant formaldehyde concentration provided by a calibration source have been recorded. The mixing ratio of formaldehyde has been adjusted to obtain an optical depth of $4 \cdot 10^{-4}$. With this constant gas mixture, a first calibration spectrum has been recorded, which has been assigned the relative concentration of unity and spectra have been recorded for about 20 min for FM spectroscopy and for the combined FM-Stark double modulation technique for about 80 min. While the drift effects caused by moving fringe structures can be clearly identified in the FM-signal, a significantly higher stability has been obtained for the sample modulation enhanced FMS signal. The stability of the measured time series concentration values has been characterized by means of the Allan variance [175]. Fig. 7 (left side) shows the FM measurement which indicates a significant decrease of the recorded time series data of the relative HCHO concentration, although a constant value would have been expected. This strong drift has been caused by the presence of fluctuating background structures. The negative influence of this signal drift finds its equivalent in the corresponding Allan plot. Up to 24 s signal averaging leads to a linear decrease of the Allan variance. Beyond this optimum integration time, the Allan variance and with it the instrument detection limit, will deteriorate as a consequence of disturbing background drifts. In contrast to this FM measurement, the relative concentration recorded with the FM-Stark modulation technique presented here exhibits almost no deviation from the expected constant value. Only a slight increment in the noise of the relative concentration values can be noticed. The Allan variance declines linearly with the integration time reflecting a white-noise dominated region. The FM-Stark double modulation technique yields an optimum integration time of 120 s which is five times the optimum integration time of the mere FM technique. Strongly correlated with this enhanced integration time is a notable gain in the Allan variance by a factor of more than three. For integration times beyond 120 s the Allan plot shows a horizontal level, which indicates the presence of $1/^{\alpha}$-type noise. Further averaging will not help to improve the detection limit. Probably this low frequency noise will be caused by the turbulent gas flow through the absorption cell which is strongly related to refractive index fluctuations. However, it was the purpose of these measurements to demonstrate the advantage of sample modulation enhanced FM spectroscopy and its ability to cope with the fringe problem and background drift.

All spectroscopic techniques, convention WMS and FMS, are limited by optical fringes and without solving the fringe problem, the potential sensitivity improvement expected from the new techniques cannot be attained on a routine basis. While the high frequency modulation of the laser allows faster measurements and reduces the noise, the sample modulation is applied to cope with the fringe problem. Therefore, it is the combination of both, laser and sample modulation, that is most promising for the future of highly specific and ultrasensitive trace gas analysis by tunable diode lasers.

5. Summary and future perspectives

In order to improve sensitivity various types of modulation spectroscopy have been employed in which the diode laser wavelength is modulated while being scanned across an absorption line. The modulation techniques allow absorptions as low as 1 part in 10^6 to be measured within a 1 Hz bandwidth. In combination with optical multipass

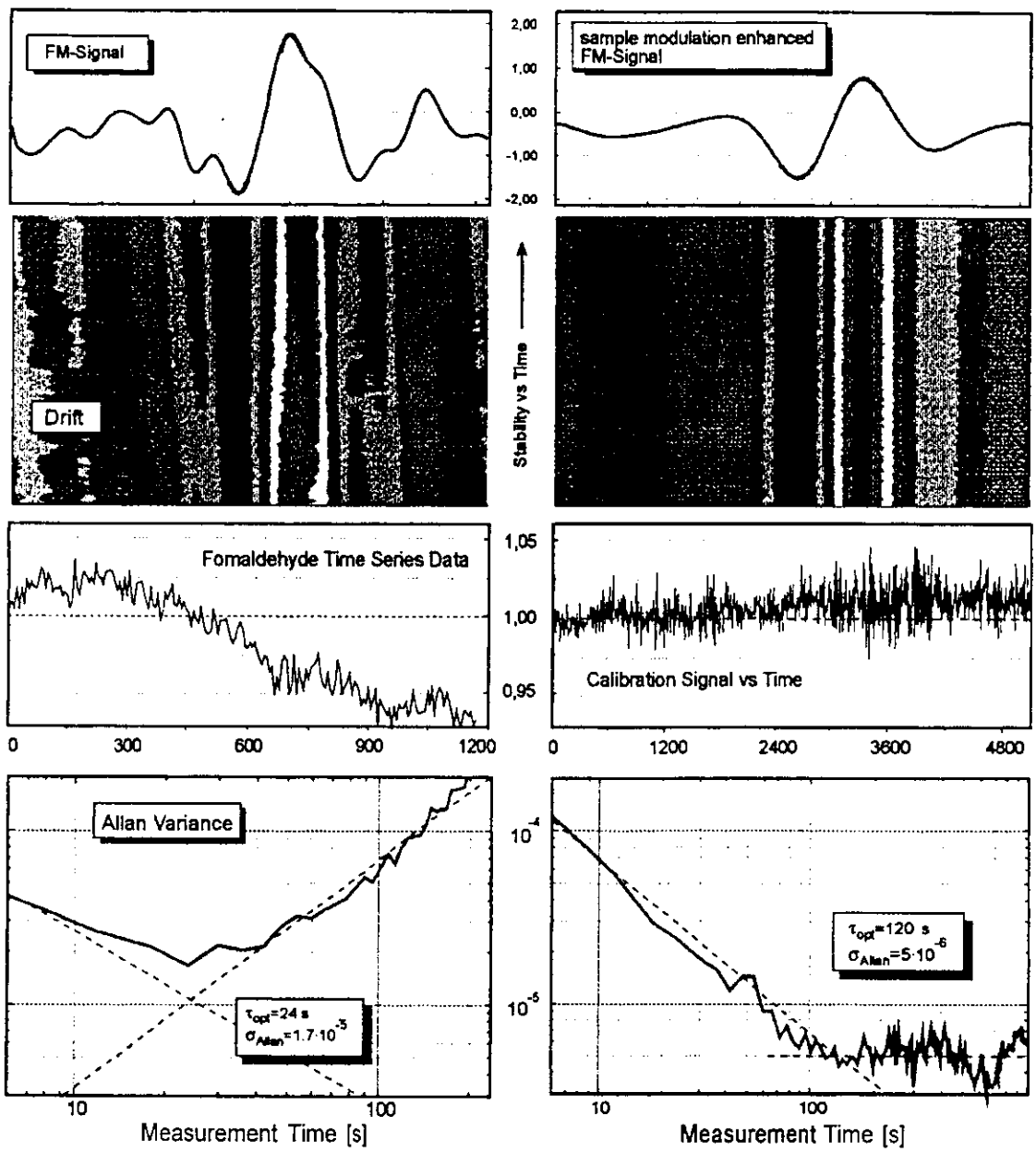

Fig. 7. Improvement of sample modulation enhanced FMS (right) vs conventional FMS (left). The increased stability is obvious in the time series data and in the Allan plots.

cells this is equivalent to detection limits of around 20 pptv for the most strongly absorbing species and better than 1 ppbv for almost all species of interest. Based on theoretical considerations and experimental demonstrations, the most efficient modulation technique depends strongly on the circumstances and cannot be stated generally. The performance will depend on system and

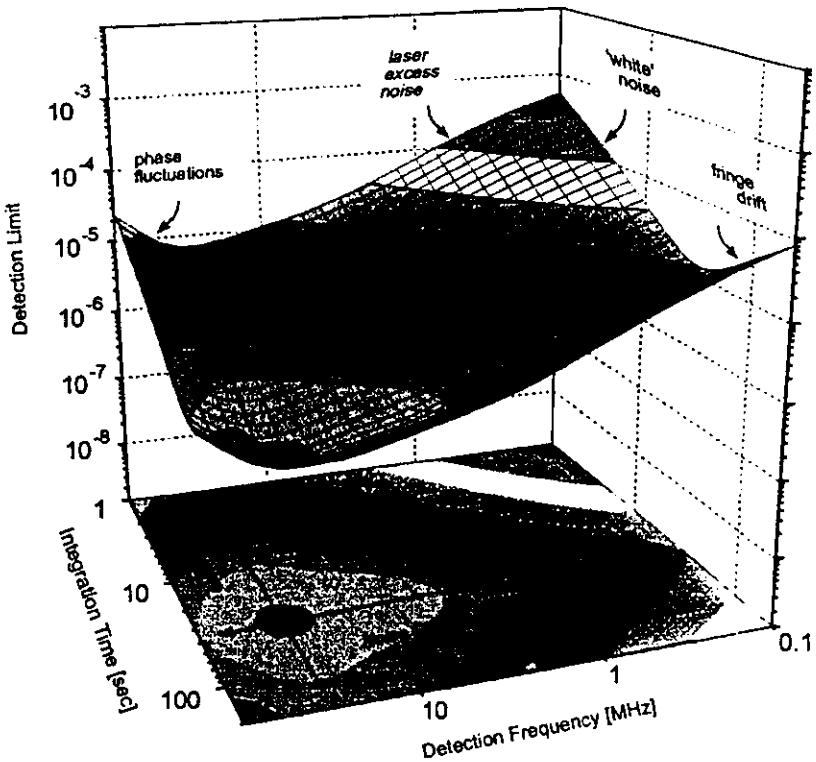

Fig. 8. Illustration of the influence of integration time and modulation/demodulation frequency on the spectrometer performance. A minimum corresponding to the current state-of-the-art near 10 MHz and 1 min averaging is indicated.

laser parameters and the actual experimental situation and spectroscopic conditions. In controlled laboratory experiments using short optical paths the high frequency techniques have been shown to be capable of quantum limited sensitivities of around $1 \cdot 10^{-7}$. However, this level of performance has yet to be demonstrated in a TDLAS instrument with long optical paths, suitable for field use over extended periods. In general, the high frequency modulation techniques appear capable of a significant improvement in TDLAS sensitivity over the WMS systems.

TDLAS has made the transition from a technique mainly of interest to instrument developers into one which produces results of real value to trace gas analysis and atmospheric chemistry studies. However, it has yet to become an instrument suited to routine use by non-expert operators, mainly due to the complex and unreproducible behavior of the lasers. Further laser development is underway to remedy this. The high frequency modulation techniques have started to produce useful measurements even if the dramatic improvements in sensitivity originally expected from these methods have not been fully realized yet. However, significant improvements in sensitivity and detection speed have been obtained.

The effects that mostly limit the ultimate sensitivity of diode laser spectrometers utilizing FM detection are summarized in Fig. 8, where the detection limit is plotted as a function of both, signal integration time and the detection frequency of the phase sensitive device. The dependence of the detection limit on the integration time has been discussed in the context of the Allan variance analysis [175] and the dependence on the detection frequency depends on the laser noise characteristics and interferometric effects [99]. One pre-requisite for ultrasensitive FM-TD-

LAS spectrometers is a laser operating in a single longitudinal mode with low noise and a high power output. The properties of lead-salt lasers presently available are far from these requirements and have to be improved substantially. The presence of even spurious side-modes leads to a significant increase in laser noise at frequencies below about 100-200 MHz. Consequently, higher modulation and detection frequencies are necessary to achieve near quantum limited performance of the FM spectrometer and for two-tone modulation, a sufficiently high difference frequency then has to be selected for detection. A second pre-requisite is a high system stability during signal averaging intervals. An FM spectrometer behaves essentially as a single beam two-color interferometer and, therefore, it is extremely sensitive to thermal drifts in the opto-mechanical setup. It can be shown that with increasing modulation frequency the sensitivity towards fluctuations in the optical path increases. While this is a great advantage for interferometric measurements, it is a great disadvantage in analytical application. Therefore, lower modulation frequencies are necessary to achieve a high degree of system stability over long averaging times. The signal instabilities at low optical densities caused by the interferometric effect may explain the fact, that the expected improvement in system performance after the application of high frequency modulation schemes to spectroscopic systems designed for conventional derivative spectroscopy has not yet been attained on a routine basis. The interferometric effect at high modulation frequencies is super-imposed on the 'etalon-effect'. When the wavelength of the diode laser is tuned over a spectral line, parasitic absorptions of resonator structures in the optical path generate a periodic fringe structure, which is superimposed on the desired signal from the absorption of the target gas. If this fringe structure is generated, say between the reflecting mirrors in the multipass absorption cell, mechanical drifts cause a change of the fringe structure. These time dependent structures are usually sensitivity limiting, if they cannot be suppressed sufficiently. But even if the optical fringes could be completely eliminated, say be removing all reflecting and transmissive optics between the laser and the detector, the 'interferometer-effect' remains. The formation of optical fringes requires reflection of laser light within resonator structures, while the interferometric effect remains even after the insertion of a perfect optical isolator in the optical path. As a conclusion, there are at least two opposing requirements for the selection of the optimum detection frequency in FM spectroscopy and with 'state of the art' FM-spectrometers, system optimization is often a trade-off between limitations due to laser excess noise and limitations caused by interferometric effects [99]. The minimum detectable absorbance can be expressed in terms of phase fluctuations or relative intensity noise. This has been done in Fig. 8 to illustrate the dependence of the detection limit as a function of both, detection frequency and signal averaging time. The levels of laser excess noise and phase fluctuations determine the initial signal-to-noise ratio for a given detection frequency prior to any signal averaging. With increasing signal averaging this level decreases until the detection limit becomes influenced by thermal drift effects. Beyond this point detection limits deteriorate again. The optimum integration time can be determined by means of the Allan variance analysis for all possible modulation frequencies. As expressed in Fig. 8, we obtain a minimum detection limit between 10^{-6} and 10^{-7} for detection frequencies around 10 MHz and integration times of about 1 min. This resembles the current state-of-the-art for typical frequency modulated spectrometer performance. Fig. 8 also gives some advice on how to improve the situation. At high modulation frequencies, an extremely high opto-mechanical stability is required, which is very expensive to obtain. However, the other direction towards lower modulation frequencies requires single mode lasers with negligible excess noise contributions. Therefore, further development and availability of high power, single mode diode lasers with distributed feedback (DFB) structures would really help to improve spectrometer performance for routine applications.

Further improvement in signal stability will allow longer integration times and, therefore,

provide better detection limits. The application of an additional sample modulation has been discussed and it has been shown that this is an efficient method for the suppression of background fluctuations and that substantial improvement of the system stability and of integration times can be achieved. The FM-Stark double modulation technique is applicable to molecules with a permanent dipole moment as NH,, HNO,, HCHO, H,O,. Other approaches are the application of the Zeeman-effect for sample modulation, which involves magnetically active molecules, with the very interesting group of radicals (e.g. HO,) among them and magnetic rotation spectroscopy, which has been successfully applied for oxygen, NO and NO,, for example. The combination of both, low noise lasers and sample modulation enhanced FM spectroscopy can cope with the background problem, at least a significant improvement of stability and, therefore, of the detection limits is expected.

Meanwhile a broad variety of diode lasers is available from the visible to the mid infrared and hopefully the spectral coverage is continuously increasing, even into the blue spectral region. It is unlikely that the near infrared diodes will ever completely replace lead-salt diodes. The two spectral regions will rather provide complementary systems. For a certain limited number of species, where ultrahigh sensitivity is not required, the near infrared systems will provide advantages of size, simplicity and cost. For other species requiring a more universal and sensitive system, the mid infrared diodes will continue to provide a superior and highly specific measurement device. Together with improved lasers and advanced signal processing technology, new sophisticated modulation schemes and optimized sample cells will allow precise and accurate trace gas analysis and lead to a continuing enhancement in sensitivity and reliability of monitoring systems as well as to a further cost reduction. However, the future development of semiconductor laser based gas monitors will be driven by new applications and measurement challenges in research and industry.

Acknowledgements

Most of this work has been funded by the German Ministry for Research and Technology (BMBF), the Bayerisches Staatsministerium fur Wirtschaft, Verkehr und Technologie and the European Community. The work of the engineers R. Konigstedt, B. Janker, K. Maurer, D. Hofmann, J. Schandl, R. Huber and the diploma and PhD students J. Wietzorrek, S. Lechner, B. Schlitt, K. Josek, B. Scheumann and R. Kormann is hereby gratefully acknowledged. I would like to thank especially Dr F. Slemr and Dr R. Miicke for many stimulating discussions and advice during the preparation of the manuscript.

References

[1] E.D. Hinkley, Appl. Phys. Lett. 16 (1970) 351.
[2] J. Reid, J. Shewchun, B.K. Garside, A.E. Ballik, Appl. Opt. 17 (1978) 300.
[3] H.I. Schiff, G.I. Mackay, J. Bechara, in: M.W. Sigrist (Ed.), Air Monitoring by Spectroscopic Techniques, Wiley, New York, 1994.
[4] D. J. Brassington, in R.E. Hester, R.J. Clark (Eds.), Advances in Spectroscopy, Spectroscopy in Environmental Science, vol. 24, Wiley, New York, 1994.
[5] H.I. Schiff (Ed.), Measurement of atmospheric gases, Proc. Sot. Photo-Opt. Instrum. Eng. 1433 (1991).
[6] R. Grisar, G. Schmidtke, M. Tacke, G. Restelli (Eds.), Monitoring of Gaseous Pollutants by Tunable Diode Lasers, Kluwer, Dordrecht, 1989.
[7] R. Grisar, H. Biittner, M. Tacke, G. Restelli (Eds.), Monitoring of Gaseous Pollutants by Tunable Diode Lasers, Kluwer, Dordrecht, 1992.
[8] A.I. Nadezdinskii, A.M. Prokhorov (Eds.), Tunable diode laser applications, Proc. Soc. Photo-Opt. Instrum. Eng. 1724 (1992).
[9] H.I. Schiff, U. Platt (Eds.), Optical methods in atmospheric chemistry, Proc.Soc. Photo-Opt. Instrum. Eng. 1715 (1993).
[10] A.W. Mantz, Microchem. J. 50 (1994) 351.
[11] M. Tacke, R. Grisar, Laser Optoelektronik 27 (1995) 51.
[12] D.E. Cooper, R.U. Martinelli, Laser Focus World 11 (1992) 133.
[13] C. Wiemann, L. Hollberg, Rev. Sci. Instrum. 62 (1991) 1.
[14] J. Lawrenz, K. Niemax, Spectrochim Acta Part B 44 (1989) 155.
[15] P. Werle, J. Physique IV (1994) 9.
[16] A. Fried (Ed.), Application of Tunable Diode Lasers and other Infrared Sources for Atmospheric Studies and

Industrial Monitoring, Proc. Soc. Photo-Opt. Instrum. Eng. 2834 (1996).
[17] R.N. Hager Jr., R.C. Anderson, J. Opt. Soc. Am. 60 (1970) 1444.
[18] J.U. White, J. Opt. Soc. Am. 66 (1976) 411.
[19] D.R. Herriott, H.J. Schulte, Appl. Opt. 4 (1964) 883.
[20] J.B. McManus, P.L. Kebabian, Appl. Opt. 29 (1990) 898.
[21] J.B. McManus, P.L. Kebabian, MS. Zahniser, Appl. Opt. 34 (1995) 3336.
[22] A. Fried, J.R. Drummond, B. Henry, J. Fox, Appl. Opt. 30 (1991) 145.
[23] H.I. Schiff, D.R. Hastie, G.I. Mackay, T. Iguchi, B.A. Ridley, Environ. Sci. Technol. 17 (1983) 5371.
[24] R.T. Menzies, E.D. Hinkley, C.R. Webster, Appl. Opt. 22 (1983) 2655.
[25] HI. Schiff, D.R. Karecki, G.W. Harris, J. Geophys. Res. 95D (1990) 10147.
[26] F. Slemr, G.W. Harris, D.R. Hastie, G.I. Mackay, H.I. Schiff, J. Geophys. Res. 91 (1986) 537 1.
[27] G.W. Sachse, G.F. Hill, L.O. Wade, M.G. Perry, J. Geophys. Res. 92 (1987) 2071.
[28] G. Schmidtke, W. Kohn, U. Klocke, M. Knothe, W.J. Riedel, H. Wolf, Appl. Opt. 28 (1990) 3665.
[29] G.W. Harris, D. Klemp, T. Zenker, J.P. Burrows, B. Mathieu, J. Atmos. Chem. 15 (1992) 315.
[30] P. Bergamaschi, M. Schupp, G.W. Harris, Appl. Opt. 33 (1994) 7704.
[31] C.R. Webster, R.D. May, C.A. Trimble, R.G. Chave, J. Kendall, Appl. Opt. 33 (1994) 454.
[32] G.I. Mackay, D.R. Karecki, H.I. Schiff, J. Geophys. Res. 101 (1996) 14721.
[33] G. Baldachini, F. D'Amato, M. de Rosa, Infrared Phys. Technol. 37 (1996) 1.
[34] A. Fried, S. Sewell, B. Henry, B.P. Wert, T. Gilpin, J. Drummond, J. Geophys. Res. 102 (1997) 6253.
[35] P. Werle, in: G. Harding, R. Lanza, L.J. Myers, P.A. Young (Eds.), Substance detection systems, Proc. Soc. Photo-Opt. Instrum. Eng. 2092 (1994) 4.
[36] P. Werle, R. Mücke, in: P. Fabian, V. Klein, M. Tacke, K. Weber, C. Werner (Eds.), Air pollution and visibility measurements, Proc. Soc. Photo-Opt. Instrum. Eng. 2506 (1995) 708.
[37] I.J. Simpson, G.W. Thurtell, G.E. Kidd, M. Lin, T.H. Demetriades-Shah, I.D. Flitcroft, E.T. Kanemasu, D. Nie, K.F. Bronson, H.U. Neue, J. Geophys. Res. 100 (1995) 7283.
[38] F.G. Wienhold, H. Frahm, G.W. Harris, J. Geophys. Res. 99 (1994) 16557.
[39] K.J. Hargreaves, U. Skiba, D. Fowler, J. Arah, F.G. Wienhold, L. Klemedtsson, B. Galle, J. Geophys. Res. 99 (1994) 16569.
[40] M.S. Zahniser, D.D. Nelson, J.B. McManus, P.L. Kebabian, Philos. Trans. R. Soc. London Ser. A 351 (1995) 371.
[41] D.P. Billesbach, F.G. Ullmann, S.B. Verma, in: A. Fried (Ed.), Application of Tunable Diode Lasers and other Infrared Sources for Atmospheric Studies and Industrial Monitoring, Proc. Soc. Photo-Opt. Instrum. Eng. 2834 (1996) 187.
[42] N. Anselm, Th. Giesen, M. Harter, R. Schieder, G. Winnewisser, in: R. Grisar, H. Böttner, M. Tacke, G. Restelli (Eds.), Monitoring of Gaseous Pollutants by Tunable Diode Lasers, Kluwer, Dordrecht, 1992, 231 pp.
[43] T. Giesen, R. Schieder, G. Winnewisser, K.M.T. Yamada, J. Mol. Spectrosc. 153 (1992) 496.
[44] M. Mürtz, M. Schafer, S. König, W. Urban, Infrared Phys. Technol. 37 (1996) 109.
[45] A.I. Nadezhdinskii, Spectrochim. Acta Part A 52 (1996) 1041.
[46] C.D. Ball, F.C. de Lucia, D. Risal, A. Ruth, H. Sheng, Y. Abebe, P.A. Farina, A.W. Mantz, in: A. Fried (Ed.), Application of Tunable Diode Lasers and other Infrared Sources for Atmospheric Studies and Industrial Monitoring, Proc. Soc. Photo-Opt. Instrum. Eng. 2834 (1996) 102.
[47] F. Taucher, C. Weitkamp, W. Michaelis, H.K. Cammenga, S. Bauerecker, Infrared Phys. Technol. 37 (1996) 155.
[48] F. Taucher, C. Weitkamp, H.K. Cammenga, S. Bauerecker, Spectrochim. Acta Part A 52 (1996) 1023.
[49] M. Haverlag, E. Stoffels, W.W. Stoffels, G.M.W. Kroesen, F.J. de Hoog, J. Vat. Sci. Technol. A 12 (1994) 3102.
[50] T. Goto, Trend. Chem. Phys. 1 (1991) 69.
[51] P. Werle, Proc. 7th Int. Symp. Laser-aided Plasma Diagnostics LPAD7, Fukuoka, Japan, 1995, 184 pp.
[52] H. Wolf, W.J. Riedel, in: R. Grisar, G. Schmidtke, M. Tacke, G. Restelli (Eds.), Monitoring of Gaseous Pollutions by Tunable Diode Lasers, Reidel, Dordrecht, 1987, p. 120.
[53] H. Neckel, J. Wolfrum, Appl. Phys. B 49 (1989) 85.
[54] A. Arnold, Appl. Opt. 29 (1990) 4860.
[55] V. Ebert, V. Sick, J. Wolfrum, Tech. Mess. 7/8 (1996) 268.
[56] D.S. Baer, E.R. Furlong, R.K. Hanson, in: A. Fried (Ed.), Application of Tunable Diode Lasers and other Infrared Sources for Atmospheric Studies and Industrial Monitoring, Proc. Soc. Photo-Opt. Instrum. Eng. 2834 (1996) 205.
[57] L. Wang, G.W. Sachse, R.E. Campbell, R.E. Davis, in: R.J. Locke (Ed.), Laser Applications in Combustion and Combustion Diagnostics, Proc. Soc. Photo-Opt. Instrum. Eng. 2122 (1994) 13.
[58] J. Wormhoudt, M.S. Zahniser, D.D. Nelson, J.B. McManus, R.C. Miake-Lye, C.E. Kolb, in: R.J. Locke (Ed.), Laser Applications in Combustion and Combustion Diagnostics, Proc. Soc. Photo-Opt. Instrum. Eng. 2122 (1994) 49.
[59] P. Wiesen, J. Kleffmann, R. Kurtenbach, K.H. Becker, Infrared Phys. Technol. 37 (1996) 75.
[60] H. Klingenberg, J. Winckler, in: R. Grisar, G. Schmidtke, M. Tacke, G. Restelli (Eds.), Monitoring of

Gaseous Pollutants by Tunable Diode Lasers, Kluwer, Dordrecht, 1989, p. 108.
[61] J.A. Silver, D.J. Kane, P.S. Greenberg, Appl. Opt. 34 *(1995) 2787.*
[62] A. Armitage, Control Instrum. 4 (1997) 27.
[63] M. de Angelis, F. Martin, F.S. Pavone, G.M. Tino, M. Inguscio, in R. Grisar, H. Böttner, M. Tacke, G. Restelli (Eds.), Monitoring of Gaseous Pollutants by Tunable Diode Lasers, Kluwer, Dordrecht, 1992, p. 257.
[64] Q.V. Nguyen, R.W. Dibble, Opt. Lett. *19 (1994) 2134.*
[65] H. Riris, C.B. Carlisle, L.W. Carr, D.E. Cooper, R.U. ,Martinelli, R.J. Menna, Appl. Opt. 33 (1994) 7059.
[66] M. Phillips, Sci. Am. 7 (1992) 52.
[67] E.V. Stephanov, K.L. Moskalenko, Opt. Eng. 32 (1993) 361.
[68] K.L. Moskalenko, A.I. Nadezhdinskii, I.A. Adamovskaya, Infrared Phys. Technol. 37 (1996) 18 1.
[69] B.A. Hare, J.A. Rallis, Medical lasers and systems, Proc. Soc. Photo-Opt. Instrum. Eng. 1650 (1992) 4.
[70] D.E. Cooper, R.U. Martinelli, C.B. Carlisle, H. Riris, D.B. Bour, R.J. Menna, Appl. Opt. 32 (1993) 6727.
[71] M. Haisch, P. Hering, W. Fabinski, M. Zöchbauer, Tech. Mess. 9 (1996) 322.
[72] G. Spanner, R. Nießner, Fresenius J. Anal. Chem. 354 (1996) 306.
[73] R.S. Inman, J.J.F. McAndrew, Anal. Chem. 66 (1994) 2471.
[74] R. Kästle, R. Grisar, M. Tacke, D. Domisch, C. Scholz, Microcontamination 11 (199 1) 27.
[75] R. Miicke, B. Scheumann, K. Brenner, P. Werle, in: P.M. Borrell, T. Cvitas, W.. Seiler (Eds.), Proc. EURO-TRAC Symp. 1996, Vol. 2, Computational Mechanics Publications, Southampton, 1996, 709 pp.
[76] A. Mercado, J.P. Davies, in: G. Harding, R.C. Lanza, L.J. Myers, P.A. Young (Eds.), Substance Detection Systems, Proc. Soc. Photo-Opt. Instrum. Eng. 2092 (1994) 27.
[77] H. Riris, C.B. Carlisle, D.F. McMillen, D.E. Cooper, Appl. Opt. 35 (1996) 4694.
[78] J. Wormhoudt, J.H. Shorter, J.B. McManus, P.L. Kebabian, MS. Zahniser, W.M. Davis, E.R. Cespedes, C.E. Kolb, Appl. Opt. 35 (1996) 3992.
[79] H.I. Schiff, S.D. Nadler, J.T. Pisano, G.I. Mackay, in: A. Fried (Ed.), Application of Tunable Diode Lasers and other Infrared Sources for Atmospheric Studies and Industrial Monitoring, Proc. Soc. Photo-Opt. Instrum. Eng. 2834 (1996) 198.
[80] H.I. Schiff, J. Bechara, J.T. Pisano, G.I. Mackay, Proc. Int. Specialty Conf. Optical Sensing for Environmental Monitoring, Air and Waste Management Association, SP-89, 1994, 921 pp.
[81] R.U. Martinelli, Laser Focus World 3 (1996) 77.
[82] R.U. Martinelli, R. J. Menna, P. K. York, D.Z. Gabuzov, H. Lee, J. Abeles, N.A. Morris, J.C. Conolly, S.Y. Narayan, J.S. Vermaak, G.H. Olsen, D.E. Cooper, C.B. Carlisle, H. Riris, in: A. Fried (Ed.), Application of Tunable Diode Lasers and other Infrared Sources for Atmospheric Studies and Industrial Monitoring, Proc. Soc. Photo-Opt. Instrum. Eng. 2834 (1996) 2.
[83] A. Popov, A. Baranov, V. Sherstnev, Y. Yakovlev, B. Scheumann, R. Mücke, P. Werle, Infrared Phys. Technol. 37 (1996) 117.
[84] A. Popov, V. Sherstnev, Y. Yakovlev, R. Miicke, P. Werle, Spectrochim. Acta Part A 52 (1996) 863.
[85] A. Popov, V. Sherstnev, Y. Yakovlev, R. Miicke, P. Werle, Spectrochim. Acta Part A 52 (1996) 2790.
[86] R.S. Eng, J.F. Butler, K.J. Linden, Opt. Eng. 19 (1980) 945.
[87] H. Preier, Appl. Phys. 20 (1979) 189.
[88] D.L. Wall, in: H.I. Schiff (Ed.), Measurement of atmospheric gases, Proc. Soc. Photo-Opt. Instrum. Eng. 1433 (1991) 94.
[89] M. Tacke, in: R. Grisar, G. Schmidtke, M. Tacke, G. Restelli (Eds.), Monitoring of Gaseous Pollutants by Tunable Diode Lasers, Kluwer, Dordrecht, 1989, p. 103.
[90] M. Tacke, Infrared Phys. Technol. 36 (1995) 447.
[91] Z. Fait, D. Kostyk, R. Woods, P. Mak, IEEE Photonics Tech. Lett. 2 (1990) 860.
[92] Z. Feit, P. Mak, R. Woods, M. McDonald, Spectrochim. Acta Part A 52 (1996) 851.
[93] A.P. Shotov, Yu.G. Selivanov, Semicond. Sci. Technol. 5 (1990) 27.
[94] R.S. Eng, A.W. Mantz, T.R. Todd, Appl. Opt. 18 (1979) 1088.
[95] P. Werle, F. Slemr, M. Gehrtz, Chr. Bräuchle, Appl. Opt. 28 (1989) 1638.
[96] H. Fischer, M. Tacke, J. Opt. Soc. Am. B 8 (1991) 1824.
[97] H. Fischer, H. Wolf, B. Halford, M. Tacke, Infrared Phys. Technol. 31 (1991) 381.
[98] C.N. Harward, J.M. Hoell, Appl. Opt. 18 (1979) 3978.
[99] P. Werle, Appl. Phys. B 60 (1995) 499.
[100] H. Wenz, R. Großkloß, W. Demtröder, Laser Optoelectronik 28 (1996) 58.
[101] L. Ricci, M. Weidemüller, T. Esslinger, A. Hemmerich, C. Zimmermann, V. Vuletic, W. König, T.W. Hänsch, Optics Commmun. 117 (1995) 541.
[102] D.B. Oh, D.C. Hovde, Appl. Opt. 34 (1995) 7002.
[103] D.M. Sonnenfroh, M.G. Allen, Appl. Opt. 36 (1997) 3298.
[104] K.J. Ebeling, B. Möller, G. Reiner, U. Fiedler, R. Michalzik, B. Weigl, C. Jung, E. Zeeb, in: W. Waidelich, H. Hügel, H. Opower, H. Tiziani, R. Wallenstein, W. Zinth (Eds.), Lasers in Research and Engineering, Springer, Heidelberg, 1996, 783 pp.
[105] D.C. Hovde, C.A. Parsons, Appl. Opt. 36 (1997) 1135.
[106] G.C. Bjorklund, Opt. Lett. 5 (1980) 15.
[107] G.C. Bjorklund, M.D. Levenson, W. Lenth, C. Oritz, Appl. Phys. B 32 (1983) 145.
[108] W. Lenth, Opt. Lett. 8 (1983) 575.
[109] W. Lenth, IEEE J. Quantum Electron. QE-20 (1984) 1045.
[110] M. Gehrtz, G.C. Bjorklund, E.A. Whittaker, J. Opt. Soc. Am. B 2 (1985) 1510.
[111] W. Lenth, M. Gehrtz, Appl. Phys. Lett. 47 (1985) 1263.

[112] M. Gehrtz, W. Lenth, A.T. Young, H.S. Jonston, Opt. Lett. 11 (1986) 132.
[113] S. Kobayashi, Y. Yamamoto, M Ito, T. Kimura, IEEE J. Quantum Electron. QE-18 (1982) 582.
[114] KY. Lau, A. Yariv, IEEE J. Quantum Electron. QE-21 (1985) 121.
[115] KY. Lau, Ch. Harder, A. Yariv, Appl. Phys. Lett. 44 (1984) 273.
[116] C.H. Henry, IEEE J. Quantum Electron. QE-18 (1982) 259.
[117] M. Osinsky, J. Buus, IEEE J. Quant. Elect. QE-23 (1987) 9.
[118] P. Werle, F. Slemr, M. Gehrtz, Chr. Bräuchle, Appl. Phys. B 49 (1989) 99.
[119] P. Werle, Spectrochim Acta Part A 52 (1996) 805.
[120] N.-Y. Chou, G.W. Sachse, Appl. Opt. 26 (1987) 3584.
[121] D.E. Cooper, T.F. Gallagher, Appl. Opt. 24 (1985) 1327.
[122] G.R. Janik, C.B. Carlisle, T.F. Gallagher, J. Opt. Soc. Am. B 3 (1986) 1070.
[123] D.E. Cooper, R.E. Warren, J. Opt. Soc. Am. B 4 (1987) 470.
[124] D.E. Cooper, R.E. Warren, Appl. Opt. 26 (1987) 3726.
[125] D.E. Cooper, C.B. Carlisle, Opt. Lett. 13 (1988) 719.
[126] J.A. Silver, A.C. Stanton, Appl. Opt. 27 (1988) 4438.
[127] J.A. Silver, Appl. Opt. 31 (1992) 707.
[128] C.B. Carlisle, D.E. Cooper, H. Preier, Appl. Opt. 28 (1989) 2567.
[129] D.E. Cooper, J.P. Watjen, Opt. Lett. 11 (1986) 606.
[130] F.S. Pavone, M. Inguscio, Appl. Phys. B 56 (1993) 118.
[131] J.M. Supplee, E.A. Whittaker, W. Lenth, Appl. Opt. 33 (1994) 6294.
[132] V.G. Avetisov, P. Kauranen, Appl. Opt. 35 (1996) 4705.
[133] C.R. Webster, R.T. Menzies, E.D. Hinkley, in: R.M. Measures (Ed.), Laser Remote Chemical Analysis, Wiley, New York, 1988, 163 pp.
[134] J. Humlicek, J. Quant. Radiat. Trans. 27 (1982) 437.
[135] M.S. Zahniser, K.E. McCurdy, A.C. Stanton, J. Phys. Chem. 93 (1989) 1065.
[136] H.E. Hunziker, H.R. Wendt, J. Chem. Phys. 60 (1974) 4622.
[137] H.E. Hunziker, H.R. Wendt, J. Chem. Phys. 64 (1976) 3488.
[138] L.S. Rothman, R.R. Gamache, A. Goldman, L.R. Brown, R.A. Toth, H.M. Picket, R.L. Poynter, J.-M. Flaud, C. Camy-Peyret, A Barbe, N. Husson, C.P. Rinsland, M.A.H. Smith, Appl. Opt. 26 (1987) 4058.
[139] L.S. Rothman, R.R. Gamache, R.H. Tipping, C.P. Rinsland, M.A.H. Smith, D.C. Brenner, V. Malathy Devi, J.-M. Flaud, C. Camy-Peyret, A. Perrin, A. Goldman, S.T. Massie, L.R. Brown, R.A. Toth, J. Quant. Spectrosc. Radiat. Trans. 48 (1992) 469.
[140] P. Werle, F. Slemr, Appl. Opt. 30 (1991) 430.
[141] D.S. Bomse, J.A. Silver, A.C. Stanton, Appl. Opt. 31 (1992) 718.
[142] T.J. Johnson, F.G. Wienhold, J.P. Burrows, G.W. Harris, Appl. Opt. 30 (1990) 407.
[143] T.J. Johnson, F.G. Wienhold, J.P. Burrows, G.W. Harris, H. Burkhard, J. Phys. Chem. 95 (1991) 6499.
[144] T.J. Johnson, F.G. Wienhold, J.P. Burrows, G.W. Harris, H. Burkhard, in: R. Grisar, H. Böttner, M. Tacke, G. Restelli (Eds.), Monitoring of Gaseous Pollutants by Tunable Diode Lasers, Kluwer, Dordrecht, 1992, p. 183.
[145] C.B. Carlisle, D.E. Cooper, Appl. Phys. Lett. 56 (1990) 805.
[146] H. Riris, C.B. Carlisle, L.W. Carr, D.E. Cooper, R.U. Martinelli, R.J. Menna, Appl. Opt. 33 (1994) 7059.
[147] J.A. Silver, D.C. Hovde, Rev. Sci Instrum. 65 (1994) 1691.
[148] P. Kauranen, I. Harwigsson, B. Jönsson, J. Chem. Phys. 98 (1994) 1411.
[149] J. Roths, R Busen, Infrared Phys. Technol. 37 (1996) 33.
[150] D.E. Cooper, R.U. Martinelli, C.B. Carlisle, H. Riris, D.B. Bour, R.J. Menna, Appl. Opt. 32 (1993) 6727.
[151] T. Güllük, H.E. Wagner, F. Slemr, Rev. Sci. Instrum. 68 (1997) 230.
[152] R. Mücke, F. Slemr, P. Werle, in: P.M. Borrell (Ed.), Proc. EUROTRAC Symposium 1994, SPB Academic Publishing bv, The Hague, The Netherlands, 1994, p. 915.
[153] R. Mücke, B. Scheumann, F. Slemr, P. Werle, in: H.I. Schiff, A. Fried, D. Killinger (Eds.), Tunable Diode Laser Spectroscopy, Lidar, and DIAL techniques Proc. Sot. Photo-Opt. Instrum. Eng. 2112 (1994) 87.
[154] R. Mücke, J. Dietrich, B. Scheumann, F. Slemr, J. Slemr, P. Werle, in: P.M. Borrell (Ed.) Proc. EUROTRAC Symposium 1994, SPB Academic Publishing bv, The Hague, The Netherlands, 1994, p. 910.
[155] R. Mücke, B. Scheumann, J. Slemr, F. Slemr, P. Werle, Infrared Phys. Technol. 37 (1996) 29.
[156] R. Kormann, K. Maurer, R. Mücke, F. Slemr, P. Werle, R. Zitzelsberger, U. Parchatka, T. Zenker, D. Trapp, H. Fischer, in: P.M. Borrell (Ed.) Proc. EUROTRAC Symposium 1996, Computational Mechanics Publications, Southampton, 1996, p. 715.
[157] F.G. Wienhold, H. Fischer, G.W. Harris, Infrared Phys. Technol. 37 (1996) 67.
[158] P. Werle, in: A.I. Nadezhdinskii, Y.N. Ponomarev, L.N. Sinitsa (Ed.), 1 lth Symp. School on High-Resolution Molecular Spectroscopy Proc. Soc. Photo-Opt. Instrum. Eng. 2205 (1994) 83.
[159] R. Kormann, PhD Thesis, University of Munich, Germany, 1997.
[160] R. Mücke, P. Werle, F. Slemr, W. Prettl, in: H.I. Schiff (Ed.), Measurement of atmospheric gases Proc. Soc. Photo-Opt. Instrum. Eng. 1433 (1991) 136.
[161] R. Mücke, P. Werle, F. Slemr, in: P.M. Borrell (Ed.), Proc. EUROTRAC Symposium 1992, Garmisch-Partenkirchen, SPB Academic Publishing bv, The Hague, The Netherlands, 1993, p.245.
[162] H. Fischer, P. Bergamaschi, F.G. Wienhold, T. Zenker, G.W. Harris, in: A Fried (Ed.), Application of Tunable Diode Lasers and other Infrared Sources for Atmo-

spheric Studies and Industrial Monitoring, Proc. Sot. Photo-Opt. Instrum. Eng. 2834 (1996) 130.
[163] H.I. Schiff, G.I. Mackay, S.D. Nadler, Infrared Phys. Technol. 37 (1996) 39.
[164] A.C. Stanton, J.A. Silver, D.S. Bomse, D.B. Oh, D.C. Hovde, M.E. Paige, D. J. Kane, in: A. Fried (Ed.), Application of Tunable Diode Lasers and other Infrared Sources for Atmospheric Studies and Industrial Monitoring, Proc. Sot. Photo-Opt. Instrum. Eng. 2834 (1996) 41.
[165] F. D'Amato, A. Lancia, P. Werle, in: A. Fried (Ed.), Application of Tunable Diode Lasers and other Infrared Sources for Atmospheric Studies and Industrial Monitoring, Proc. Sot. Photo-Opt. Instrum. Eng. 2834 (1996) 242.
[166] C.R. Webster, J. Opt. Sot. Am. 2 (1985) 1464.
[167] J.A. Silver, A.C. Stanton, Appl. Opt. 27 (1988) 1914.
[168] D.T. Cassidy, J. Reid, Appl. Phys. B 29 (1982) 279.
[169] H.C. Sun, E.A. Whittaker, Appl. Opt. 31 (1992) 4998.
[170] P. Werle, in: H.I. Schiff, A. Fried, D. Killinger (Eds.), Tunable Diode Laser Spectroscopy, Lidar, DIAL techniques, Proc. Sot. Photo-Opt. Instrum. Eng. 2112 (1994) 19.
[171] H. Riris, C.B. Carlisle, R.E. Warren, Appl. Opt. 33 (1994) 5506.
[172] P. Werle, B. Scheumann, J. Schandl, Opt. Eng. 33 (1994) 3093.
[173] H. Riris, C.B. Carlisle, R.E. Warren, D.E. Cooper, Opt. Lett. 19 (1994) 144.
[174] H. Riris, C.B. Carlisle, R.E. Warren, D.E. Cooper, R.U. Martinelli, R.J. Menna, PK. York, D.Z. Garbuzov, H. Lee, J.H. Abeles, N. Morris, J.C. Connolly, S.Y. Narayan, Spectrochim. Acta Part A 52 (1996) 835.
[175] P. Werle, R. Mticke, F. Slemr, Appl. Phys. B 57 (1993) 131.
[176] P. Werle, Infrared Phys. Technol. 37 (1996) 59.
[177] P. Werle, B. Janker, Opt. Eng. 35 (1996) 2051.
[178] P. Werle, B. Janker, Tech. Mess. 63 (1996) 92.
[179] E.A. Whittaker, H.R. Wendt, H.E. Hunziker, G.C. Bjorklund, Appl. Phys. B 35 (1984) 105.
[180] J.M. Smith, J.C. Bloch, R.W. Field, J.I. Steinfeld, J. Opt. Sot. Am. 12 (1995) 964.
[181] T.A. Blake, C. Chackerian, J.R. Podolske, Appl. Opt. 35 (1996) 973.
[182] R.J. Brecha, L.M. Pedrotti, D. Krause, J. Opt. Sot. Am. B, 1997.
[183] P. Werle, S. Lechner, in: A. Fried (Ed.), Application of Tunable Diode Lasers and other Infrared Sources for Atmospheric Studies and Industrial Monitoring, Proc. Sot. Photo-Opt. Instrum. Eng. 2834 (1996) 68.